HHS Public Access

Author manuscript

J Neurochem. Author manuscript; available in PMC 2017 March 06.

Published in final edited form as:

J Neurochem. 2017 March ; 140(6): 919–940. doi:10.1111/jnc.13950.

Identification of altered brain metabolites associated with TNAP activity in a mouse model of hypophosphatasia using untargeted NMR-based metabolomics analysis

Thomas Cruz[1], **Marie Gleizes**[2], **Stéphane Balayssac**[1], **Etienne Mornet**[3], **Grégory Marsal**[2], **José Luis Millán**[4], **Myriam Malet Martino**[1], **Lionel G Nowak**[2], **Véronique Gilard**[1], and **Caroline Fonta**[2,*]

[1]Groupe de RMN Biomédicale, Laboratoire SPCMIB (CNRS UMR 5068), Université Paul Sabatier, Université de Toulouse, 118 route de Narbonne, 31062 Toulouse cedex, France.

[2]Centre de Recherche Cerveau et Cognition (CerCo), Université de Toulouse UPS; CNRS UMR 5549, Toulouse, France.

[3]Unité de Génétique Constitutionnelle Prénatale et Postnatale, Service de Biologie, Centre Hospitalier de Versailles, 78150 Le Chesnay, France.

[4]Sanford Burnham Prebys Medical Discovery Institute, La Jolla, California, USA.

Abstract

Tissue Nonspecific Alkaline Phosphatase (TNAP) is a key player of bone mineralization and TNAP gene (*ALPL*) mutations in human are responsible for hypophosphatasia (HPP), a rare heritable disease affecting the mineralization of bones and teeth. Moreover, TNAP is also expressed by brain cells and the severe forms of HPP are associated with neurological disorders, including epilepsy and brain morphological anomalies. However TNAP's role in the nervous system remains poorly understood. In order to investigate its neuronal functions, we aimed to identify without any a priori the metabolites regulated by TNAP in the nervous tissue. For this purpose we used ^{1}H- and ^{31}P NMR to analyze the brain metabolome of *Alpl* (*Akp2*) mice null for TNAP function, a well-described model of infantile HPP. Among 39 metabolites identified in brain extracts of one week-old animals, 8 displayed significantly different concentration in $Akp2^{-/-}$ compared to $Akp2^{+/+}$ and $Akp2^{+/-}$ mice: cystathionine, adenosine, GABA, methionine, histidine, 3-methylhistidine, N-acetylaspartate (NAA) and N-acetyl-aspartyl-glutamate (NAAG), with cystathionine and adenosine levels displaying the strongest alteration. These metabolites identify several biochemical processes that directly or indirectly involve TNAP function, in particular through the regulation of ecto-nucleotide levels and of pyridoxal phosphate-dependent enzymes. Some of these metabolites are involved in neurotransmission (GABA, adenosine), in myelin synthesis (NAA, NAAG), and in the methionine cycle and transsulfuration pathway

*Corresponding author, caroline.fonta@cnrs.fr.

ARRIVE guidelines have been followed:
Yes => if No, skip complete sentence => if Yes, insert "All experiments were conducted in compliance with the ARRIVE guidelines."

Conflicts of interest: none => if 'none', insert "The authors have no conflict of interest to declare." => otherwise insert info unless it is already included

(cystathionine, methionine). Their disturbances may contribute to the neurodevelopmental and neurological phenotype of HPP.

Keywords

tissue nonspecific alkaline phosphatase; MSCA-1; pyridoxal phosphate; cystathionine; nucleotide; neuron

Introduction

The ubiquitous expression of Alkaline Phosphatase (AP, EC 3.1.3.1) has been largely demonstrated among the vertebrate and invertebrate phyla (Yang *et al.* 2012; Zimmermann *et al.* 2012). Tissue Nonspecific Alkaline Phosphatase (TNAP) is one of the AP isozymes found in vertebrates. In mammals, it is expressed as isoforms in tissues such as bone, cartilage, kidney, liver, lung, as well as in the brain (*e.g.*, (Brun-Heath *et al.* 2011; Buchet *et al.* 2013; Hoshi *et al.* 1997; Weiss *et al.* 1988)). In adult brains, blood vessels are nicely delineated by the AP activity of endothelial cells, (e. g. (Anstrom *et al.* 2002; Bell and Ball 1985; Fonta and Imbert 2002; Newman *et al.* 1950)). AP activity has also been demonstrated in adult brain parenchyma (Shimizu 1950), where its spatial distribution displays species-specific patterns (e.g.(Fonta *et al.* 2004; Friede 1966; Kantor *et al.* 2015; Langer *et al.* 2008; Negyessy *et al.* 2011)). Electron microscopy studies further showed dense AP activity at sites of synaptic connections and on nodes of Ranvier (Fonta *et al.* 2004; 2005; Mori and Nagano 1985; Pinner *et al.* 1964; Sugimura and Mizutani 1979). This activity is displayed on the extracellular side of the cell membrane, giving TNAP its status of ectoenzyme (*e. g.* (Fedde and Whyte 1990; Fonta *et al.* 2004; Mayahara *et al.* 1967)).

TNAP activity is also strongly associated with brain development. Strong TNAP activity is observed in cerebral regions of increased proliferative activity such as the ventricular zones (Langer *et al.* 2007; Narisawa *et al.* 1994). Studies also suggested that TNAP participates to neuronal differentiation and axonal growth (Diez-Zaera *et al.* 2011; Ermonval *et al.* 2009; Kermer *et al.* 2010) and that it is involved in myelination and synaptogenesis (Fonta *et al.* 2005; Hanics *et al.* 2012; Narisawa *et al.* 1997).

These results suggest that TNAP plays important roles in brain development and functioning. This hypothesis is corroborated by observations collected from humans with TNAP mutations leading to the severe forms of HPP (Greenberg *et al.* 1993; Rathbun 1948; Taillandier *et al.* 2005; Taketani 2015; Weiss *et al.* 1988) and from mice in which TNAP gene function has been ablated (Narisawa *et al.* 1997; Waymire *et al.* 1995): a neurological phenotype, mainly characterized by epileptic seizures, is observed in both case. In patients with the severe perinatal form of HPP, cerebral imaging revealed, among others, hypodensity of the white matter and dilated ventricles, thereby adding convincing evidence that TNAP malfunction directly impacts brain structure (de Roo *et al.* 2014; Demirbilek *et al.* 2012; Hofmann *et al.* 2013; Nunes *et al.* 2002).

Although clinical and experimental studies support the hypothesis that TNAP contributes to the development and functioning of the nervous system, a more complete understanding of

the roles of this enzyme requires examining its functions at the molecular level. Studies in other tissues have revealed several TNAP substrates, whose levels are increased in HPP patients and TNAP-knockout mice. Historically, phosphoethanolamine (PE) was the first compound associated with HPP as its plasmatic and urinary concentrations were found to be considerably increased in HPP patients (Fraser *et al.* 1955; McCance *et al.* 1955). Likewise, urinary PE levels are also elevated in TNAP-knockout mice (Fedde *et al.* 1999). Inorganic pyrophosphate (PPi), a key player in bone mineralization (Harmey *et al.* 2004), is also a substrate of TNAP as it is found in higher concentrations in HPP patients (Russell 1965) as well as in TNAP-knockout mice (Fedde *et al.* 1999). Finally, pyridoxal phosphate (PLP), the major form of vitamin B6, accumulates in the serum of both HPP patients (Whyte *et al.* 1988; Whyte *et al.* 1985) and TNAP-knockout mice (Waymire *et al.* 1995). TNAP hydrolyzes extracellular PLP into pyridoxal (PL), which can passively diffuse through the cell membrane (reviewed in (Coburn 2015)). Within the cells, PL is rephosphorylated to PLP, which is used as co-factor of numerous enzymatic reactions (>60 in mammals (Percudani and Peracchi 2009)). Among these so-called B6-enzymes, some are involved in the metabolism of neurotransmitters, biogenic amines and sphingolipids. Thus in the brain, TNAP dysfunction has consequences on GABA, serotonin and dopamine synthesis (Balasubramaniam *et al.* 2010; Fonta *et al.* 2012; Waymire *et al.* 1995).

In addition to the aforementioned PE, PPi and PLP, studies showed that TNAP is also capable hydrolyzing extracellular adenine nucleotides in several tissues such as airways, bone or liver (e. g.,(Ciancaglini *et al.* 2010; Picher *et al.* 2003; Say *et al.* 1991; van Belle 1976)). TNAP may also act as an ectonucleotidase in the nervous system (Diez-Zaera *et al.* 2011; Dorai and Bachhawat 1977; Ohkubo *et al.* 2000; Street *et al.* 2013). It may thus modulate the extracellular ATP/adenosine ratio and affect cellular processes of brain development, neurotransmission and neuroinflammation, via purinergic signaling regulation (Langer *et al.* 2008; Pike *et al.* 2015; Street and Sowa 2015; Zimmermann 2006).

The results published thus far point toward the manifold molecular functions exerted by TNAP in the brain, but the picture remains fragmentary given the targeted experimental approaches used in the previous studies. In order to provide a more global insight, a metabolomics approach was carried out. In the last decade metabolomic studies of brain tissue or biofluids from animal models and patients have led to the identification of metabolic signatures of various neurodegenerative diseases and mental disorders ((Dumas and Davidovic 2015; Gonzalez-Riano *et al.* 2016) and references therein). Our project aimed to identify without any *a priori* the metabolites specifically altered by the lack of TNAP activity in the brain. These metabolites could be the substrates and products of TNAP itself, or substrates and products of other biochemical processes indirectly involving TNAP such as those implicating PLP-dependent enzymes. For this purpose, we compared the metabolomes of wild-type mice ($Akp2^{+/+}$, *Akp2* being the murine TNAP gene) to that of mice partially or totally deficient in TNAP activity (heterozygous $Apk2^{+/-}$ and homozygous $Akp2^{-/-}$, respectively). We used *in vitro* proton Nuclear Magnetic Resonance (^{1}H NMR) spectroscopy as the main tool. Complementary analyses were performed using phosphorus-31 Nuclear Magnetic Resonance (^{31}P NMR) and mass spectrometry (MS). Out of 39 well-identified metabolites, we found 8 (7 for the first time) that showed significantly altered concentration in the brain of TNAP-knockout mice.

Materials and Methods

Animals and sample collection

Inactivation of the TNAP gene in the mouse phenocopies severe lethal infantile HPP (Fedde *et al.* 1999; Narisawa *et al.* 1997; Waymire *et al.* 1995). *Akp2* mice (Narisawa *et al.* 1997) were bred in the CerCo animal facilities in accordance with the Guide for the Care and Use of Laboratory Animals (National Research Council 1996, European Directive 86/609) and the guidelines of the local institutional animal care and use committee. The study was approved by the Regional (Midi-Pyrénées) Ethics Committee (ref. No. MP/06/79/11/12).

In our rearing conditions, $Akp2^{-/-}$ mice do not survive beyond 8-10 days. Previous experiments have shown modifications in the growth of the cerebral white matter from 4 days of age and delayed myelination and synaptic maturation in 7-8 day-old $Akp2^{-/-}$ mice (Hanics *et al.* 2012). On the other hand, neuronal circuits and, more specifically, GABA inhibitory transmission in the cortex, are not functional before 7-8 postnatal days (PND) in mice (Daw *et al.* 2007). Therefore, the experiments were performed with 7-day-old animals.

Young animals, both males and females, were obtained from $Apk2^{+/-}$ couples that had free access to tap water and commercial solid food (CRM (E) expended, Special Diet Service) containing vitamin B6 (Pyridoxine, 18.25 mg/kg). No additional vitamin B6 was given to the adult or young mice.

All brain samples were collected in the late morning. Mice were weighed, anesthetized by hypothermia to slow down brain metabolism, and then decapitated. Brains, including olfactory bulbs, cerebral hemispheres, brain stem and cerebellum, were quickly removed, weighed, immediately frozen in liquid nitrogen and stored at −80°C.

Mice genotypes were specified *a posteriori* using tail samples. Genotyping was performed by PCR analysis of the *Akp2* region containing the 1100 bp insert in exon 6 used to inactivate the *Akp2* gene. The wild-type PCR product is expected to have a size of 187 bp while the mutant PCR product with an insert has a size of 1287 bp. Briefly, 10-50 ng of genomic DNA in a total volume of 20 µL were subject to 36 cycles of PCR (94°C 30 sec, 55°C 40 sec, 72°C 5 min 30 sec) by using the Promega PCR Master Mix. The sequences of oligonucleotides used to amplify the target were 5′TGCTGCTCCACTCACGTCGAT (forward) and 5′AGTCCGTGGGCATTGTGACTA (reverse). The expected sizes were 187 bp for +/+ mice, 187 bp and 1287 bp for +/− mice and 1287 bp for −/− mice.

A total of 32 mice were studied, including 11 wild-type $Akp2^{+/+}$, 12 heterozygous $Akp2^{+/-}$ and 9 homozygous knockout $Akp2^{-/-}$ mice. Except for one $Akp2^{-/-}$ mouse, the TNAP deficient animals were all from the same litters as the control mice.

Chemicals

Sodium 2,2,3,3-tetradeutero-3-trimethylsilylpropionate (TSP) and all reference compounds for NMR signal assignments (cystathionine, GABA, adenosine, serine, cysteine, homocysteine, alpha ketobutyrate, methionine, PLP, PPi) were purchased from Sigma-

Aldrich (St Louis, MO, USA). Methanol and chloroform were supplied by Carlo Erba (Val de Reuil, France).

Tissue extraction

The frozen tissues were weighed (260 ± 23 mg, mean ± SD) and the brain extracts prepared according to the procedure described by (Beckonert *et al.* 2007) using a chloroform:methanol:water mixture (2:2:1.425 (v/v/v)). The whole brain was transferred into an ice cold glass vial maintained on ice. Ultra-pure cold water (0.425 mL) and cold methanol (2 mL) were added. The suspension was pulverized with an Ultra-Turrax (IKA-Werke, Staufen, Germany) for 3 × 10 s and then sonicated with a sonicator probe (Vibra cell™, Sonic, Newtown, USA) for 3 × 10 s. Two mL of cold chloroform and 1 mL of ultra-pure cold water were then added and the mixture was vortexed for 15 s and kept on ice for 15 min. After centrifugation (15 min, 1100 × g, 5000 rpm, 4°C), the upper methanol/water phase was collected. This solution was lyophilized overnight, then suspended in 2 mL of water. 1.5 mL were collected for NMR analysis and 0.5 mL withdrawn for MS investigations. After analysis, all samples were dried anew by speed vacuum centrifugation for 8 h, lyophilized overnight and stored at −80°C.

^{1}H NMR spectroscopy

550 μL of borate buffer in D_2O at pH 10 were added to the lyophilized sample (final concentration 62.5 mM) and 5 μL of a 5 mM solution (25 nmol) of TSP were added as an internal chemical shift and quantification reference. Using a pH of 10 allowed resolving several resonances that overlap at pH 7, taking advantage of chemical shift variations of NMR signals from metabolites with ionisable groups such as aminoacids, amines, or organic acids with pH (Robert *et al.* 2011). The quality of the extraction protocol in the chosen conditions and the stability of brain metabolites at pH 10 have previously been demonstrated (Lalande *et al.* 2014).

The solution was then transferred into a 5 mm diameter NMR tube and ^{1}H NMR spectra were recorded on a Bruker Avance spectrometer (Bruker Biospin AG, Fallanden, Switzerland) operating at 400.13 MHz and equipped with a 5 mm broadband inverse probe. ^{1}H NMR experiments were acquired at 298 K using a classical 1D pulse sequence (relaxation delay-pulse-acquisition), a 2.0 s pre-saturation pulse for water (HOD) signal suppression, and a repetition time of 5.7 s. A flip angle of 30° was used with 32K data points for acquisition over a spectral width of 11 ppm (4400 Hz) and 768 scans were collected.

Data were processed using the Bruker TopSpin 3.2 software with one level of zero-filling and Fourier transformation after multiplying the FIDs by an exponential line-broadening function of 0.3 Hz. Phase adjustment of NMR signals and baseline correction using the sine function tool included in the TopSpin software were done manually on each spectrum. Under these recording conditions, all ^{1}H resonances were fully relaxed as previously reported (Lalande *et al.* 2014).

Metabolite identities were assigned with an in-house metabolite database at pH 10 and with a public database (Wishart *et al.* 2013). Pure standard compounds (cystathionine, homocysteine, serine, alpha ketobutyrate, cysteine, adenosine, GABA, methionine, PLP)

were added to the analyzed extracts for confirming assignments for regions presenting strong overlap between signals or for checking suitability of signal detection for metabolites that were not detected in the brain extracts. Signals used for quantification were chosen after their assignments based on previous studies (Robert *et al.* 2011) and/or comparison with in-house metabolite database.

The selective ^{1}H 1D COSY experiments (selcogp) were performed on cystathionine NMR signals with an off-resonance 180° pulse of 118.5 ms (GausCascadeG3, 256 points). The parameters were: relaxation delay 1 s, acquisition time 1.64 s (32K data points), spectral width of 20 ppm (8000 Hz) and 1024 or 2048 scans. The transmitter frequency offset (o1p) was adjusted at 3.9 or 4.7 ppm depending on the selective excitation.

^{31}P NMR spectroscopy

^{1}H-decoupled ^{31}P NMR spectra were recorded without nuclear Overhauser effect using the same Bruker Avance spectrometer operating at 161.99 MHz and equipped with a TBO probe. Spectra were acquired by re-analyzing the solutions used for ^{1}H NMR except that 5 mg of the paramagnetic agent chromium(III) acetylacetonate were added to shorten the T1 relaxation times of the phosphorylated compounds as well as 20 µL of a 5 mM solution of an internal reference (methylene diphosphonic acid) which was used as chemical shift reference and calibrated at 16.30 ppm. Spectra were recorded under the following instrumental conditions: sweep width, 270 ppm; flip angle, 30°; repetition time, 6.54 s; 7680 scans (14 h recording). Spectra were processed by exponential multiplication with a line broadening of 3 Hz. In these experimental conditions, the detection limit is 25 µmol L^{-1} with an S/N of 3, the S/N being 2.5 × (peak height/noise height measured peak-to-peak) for a molecule containing one phosphorus atom, and 12.5 µmol L^{-1} for PPi that contains two equivalent nuclei.

Targeted UHPLC-MS/MS analysis of cystathionine

Nine samples coming from *Akp2*$^{+/+}$ (n=2), *Akp2*$^{+/-}$ (n=3) and *Akp2*$^{-/-}$ (n=4) mice previously analyzed by ^{1}H NMR were investigated. Samples withdrawn for MS analysis were suspended in 1 mL acetonitrile:water (50:50) under vortex agitation during 1 min and then sonicated for 5 min. The suspension was then centrifuged (5 min, 4000 rpm) and the supernatant analyzed after filtration using 3 kDa Amicon Ultra-0.5 ml filters (Merck Millipore) with a UHPLC Thermo Scientific Dionex UltiMate 3000 system coupled to a Q-TRAP 4500 AB Sciex (AB SCIEX, Warrington, UK) mass spectrometer. The chromatographic conditions for analysis were: C8 Symmetry® column (75 mm × 4.6 mm i.d.; 3.5 µm particle size); mobile phase: (A) demineralized water with 0.1% (v/v) formic acid and (B) methanol (HPLC grade); flow rate: 0.3 ml min^{-1}. The elution conditions were a 60:40 A:B mixture from 0 to 6 min, then a linear gradient up to 0:100 A:B from 6 to 8 min, followed by an isocratic elution during 1 min, and finally a reequilibration to 60:40 A:B mixture in 1 min. Cystathionine eluted at 2.67 min. For MS detection, the instrument parameters were as follows: for MS analysis, declustering potential (DP) 50 V and scan range m/z 160-1000; for MS/MS analysis: DP 50 V, collision energy (CE) 20 V, and scan range m/z 50-230. Detection of cystathionine was achieved by selected reaction monitoring (SRM) in positive mode using a QTrap mass spectrometer with a Turbo ion spray source at

400°C. The ion spray voltage was set at 5500 V, DP was 30 V, CE was 20 V. The monitored transition was m/z 223 ($[M+H]^+$) → 134.

Chemometric data analysis

^{1}H NMR spectra were transferred to the KnowItAll® software (Bio-Rad, Cambridge, MA, USA). The bin area method was used to segment the spectra between 0.8 and 9.3 ppm using the intelligent variable size bucketing tool included in the KnowItAll® package. Close to 600 variables were generated with one signal (or noise) per bucket. The bins of water (HOD) (4.7-5.2 ppm) and residual methanol (3.34-3.36 ppm) resonances were excluded.

A manual filtering procedure was applied to the whole spectrum to exclude buckets that contained only noise. Buckets corresponding to one metabolite were grouped when possible, according to NMR signal assignment. A total of 223 variables (buckets) were thus retained for the subsequent statistical analyses. Bin areas were integrated and transferred to the Pirouette software (Infometrics, Inc., Woodinville, WA, USA), which generated a matrix consisting of rows representing the 32 samples and columns representing the 223 variables. Integrated regions were normalized by dividing their areas by that of the internal standard TSP and by brain weight.

The statistical approach followed for metabolomics analysis has already been described (Lalande *et al.* 2014). Multivariate statistical analyses were carried out using an in-house package developed in the R environment (Balayssac *et al.* 2013) and the SIMCA-P+ 12.0 software (Umetrics, Umeå, Sweden). First, an unsupervised approach by Principal Component Analysis (PCA) was applied to the ^{1}H NMR data set. PCA was primarily used for outlier detection and for determining trends for grouping determined by mouse genotypes. Then, after Unit Variance scaling of the data in which the standard deviation of each column was used as the scaling factor, three groups corresponding to three genotypes ($Akp2^{+/+}$, $Akp2^{+/-}$, $Akp2^{-/-}$) were considered for supervised statistical analysis by Partial Least Squares Discriminant Analysis (PLS-DA) and were pairwise compared. The predictive ability of the PLS-DA models was validated by the goodness-of-fit (R^2_Y, R^2_X) and the goodness of prediction (Q^2) parameters, the response permutation test (based on 999 permutations) and the analysis of variance of the cross-validated residuals (CV-ANOVA). Loading plot, coefficient plot and variable importance in the projection (VIP) from PLS-DA models were used to identify the variables driving the separation between classes, i.e., the metabolites which can be potential biomarkers. Correlation coefficients were mainly used for the attribution of the NMR signals of cystathionine. Indeed, the Pearson's linear correlation coefficient captures linear dependency between two variables, providing, for a threshold >0.9, a statistical indicator on the structural correlations of a metabolite. Metabolites concentrations were obtained from their targeted NMR signals (Table 1) using the general equation: $C_x=(A_x/A_{TSP})\times(9/N_x)\times(n/m)$, where A_X and A_{TSP} represent the areas of the signals of the metabolite X and of TSP, respectively, 9 and N_X the number of protons of TSP and of the metabolite X, respectively, n the number of nmol of TSP in the solution, and m the brain weight (g). This quantification method has been validated in a previous publication (Robert *et al.* 2011). Metabolite concentrations were compared with non-parametric tests. For each metabolite, comparisons between the three genotypes were

performed using the Kruskal-Wallis test (p-values corrected for multiple comparisons using the Holm-Šídák procedure). Paired comparisons between groups of mice were done with the Mann-Whitney test (p-values corrected for multiple comparisons). To provide a quantitative estimate of the difference between groups, we calculated the ratio of the means, and the associated 95% confidence intervals using Fieller's method (Franz 2007).

Results

^{1}H NMR spectra and metabolite signal assignments

1D ^{1}H NMR spectra were collected from aqueous extracts of whole brains of control wild-type *Akp2*$^{+/+}$ (n=11), heterozygous *Akp2*$^{+/-}$ (n=12) and homozygous *Akp2*$^{-/-}$ (n=9) mice. A typical ^{1}H NMR spectrum of an aqueous extract of an *Akp2*$^{+/+}$ mouse brain is presented in Figure 1. Classical brain metabolites of mammals were detected, with N-acetylaspartate (NAA), creatine (Cr), lactate (Lac), taurine (Tau) and phosphocholine (PC) generating the most prominent signals.

On visual inspection, all spectra appeared qualitatively similar, the same signals being detected for all genotypes. However, a careful inspection of some regions of the spectra revealed differences in signal intensities between wild-type, heterozygous and knockout samples. Although most differences could be attributed to resonances of assigned metabolites (see below, statistical analysis), there were nevertheless 3 regions of the spectra (around δ (ppm) 3.50, 2.88 and 2.65) where *Akp2*$^{-/-}$ brain extracts demonstrated additional or stronger signals in comparison to *Akp2*$^{+/+}$ and *Akp2*$^{+/-}$ (Figure 2A). These additional signals did not fit with those of any metabolite in our database. Statistical analyses revealed strong Pearson correlation coefficients (>0.9 ($p < 10^{-8}$)) between these signals, suggesting that they belonged to the same metabolite. This finding was confirmed with COSY selective NMR experiments that showed correlations (i) between the multiplet centered at 2.88 ppm and the signal at 3.50 ppm, (ii) between the signal at 3.50 ppm and the multiplet at 2.88 ppm and a signal centered around 2.00 ppm that overlapped with signals for glutamate and glutamine. A selective irradiation of the region centered at 2.00 ppm highlighted correlations with the triplet (t) at 2.65 ppm and the multiplet (m) at 3.50 ppm. These experiments led us to hypothesize that these unassigned NMR resonances came from cystathionine, a dipeptide formed from serine and homocysteine. This was confirmed by spiking with the authentic standard. Chemical shifts for this metabolite are δ (ppm) 3.50 (m, 2H, CH 1 and 5); 2.88 (ABd, $^{2}J_{AB}$ = 13.7 Hz, $^{3}J_{AH5}$ = 5.0 Hz, $^{3}J_{BH5}$ = 7.0 Hz, 2H, CH_2 4); 2.65 (t, 2H, ^{3}J = 7.5 Hz, CH_2 3 and 2.00 (m, 2H, CH_2 2) (see Figure 2 for numbering).

In order to confirm the presence of cystathionine with a complementary method, a targeted analysis using MS was performed by UHPLC-MS/MS with the SRM mode in order to enhance sensitivity. Conditions were first optimized using a standard solution of cystathionine. Chromatographic conditions carried out in our study were close to those from literature data for cystathionine (Bartl *et al.* 2014). The selected fragmentation for SRM was that of the pseudomolecular ion $[M+H]^+$ at m/z 223 to the main fragment at m/z 134 as shown in Figure 2B. The superimposition of representative chromatograms of brain extracts from *Akp2*$^{+/+}$, *Akp2*$^{+/-}$ and *Akp2*$^{-/-}$ mice clearly shows that the cystathionine peak, although detected in all extracts, was much higher in the brain extracts of *Akp2*$^{-/-}$ mice

(Figure 2C). Cystathionine is thus a first discriminating metabolite for knockout mice. Statistical analyses were next performed in order to identify other potential biomarkers distinguishing between groups.

Statistical analyses

A non-supervised PCA analysis was first carried out to analyze the NMR data (Figure 3A). The PCA score plot did not show dominant trends by visualization on the first and second components, which accounted for 61% and 16%, respectively, of the variance of the data. Yet a trend for a clustering of *Akp2*$^{-/-}$ mice versus other mice was observed on the third component of the PCA, although it explained only 7% of the variation. The PCA analysis indicated that the metabolome of *Akp2*$^{-/-}$ mice was distinct from that of *Akp2*$^{+/-}$ and *Akp2*$^{+/+}$ mice. A supervised analysis with PLS-DA was next performed in order to identify discriminating metabolites.

The results of the supervised PLS-DA analyses of pairwise comparisons on the 223 variables are reported in Figure 3B. Comparison between *Akp2*$^{+/+}$ and *Akp2*$^{+/-}$ resulted in a non-predictive model with 2 principal PLS components (Q^2cum=0.008 and R^2_Ycum=0.57). In contrast, comparison of *Akp2*$^{+/+}$ with *Akp2*$^{-/-}$ led to a model with 3 principal PLS components with good predictive values (Q^2cum=0.92 and R^2_Ycum=0.97). Likewise, a comparison of *Akp2*$^{+/-}$ versus *Akp2*$^{-/-}$ led to a model with 2 principal PLS components with good predictive values (Q^2cum=0.79 and R^2_Ycum=0.92). For the two comparisons with knockout mice, the p-values of the CV-ANOVA were 2.6×10^{-4} and 2.5×10^{-5}, respectively. All Q^2 and R^2 values were lower in the permutation tests than in the model, revealing great predictability and goodness of the PLS-DA models. In both comparisons, the same three most discriminating metabolites were highlighted: adenosine, GABA, and cystathionine. Boxplots of each metabolite are presented in Figure 3C, showing that adenosine and GABA levels were lower in *Akp2*$^{-/-}$ than in *Akp2*$^{+/+}$ and *Akp2*$^{+/-}$ brain extracts whereas cystathionine was more concentrated in the brain of knockout mice. Other metabolites that ranked lower in the VIP plot (not shown) are considered below. Therefore, the complete loss of TNAP activity in the cerebral tissue has significant metabolic consequences on three metabolites that objectively discriminate *Akp2*$^{-/-}$ mice from their littermates *Akp2*$^{+/-}$ and *Akp2*$^{+/+}$: adenosine, GABA and cystathionine.

^{1}H NMR absolute quantification of metabolites

In addition to cystathionine, GABA and adenosine, 36 metabolites have been unambiguously identified in the ^{1}H NMR spectra. The levels of metabolites measured in our *Akp2*$^{+/+}$ control mice are consistent with those that have been quantified in previous studies in similarly aged rodents (Huguet *et al.* 1998; Kulak *et al.* 2010; Schmitt *et al.* 2013).

The mean concentrations of the 39 metabolites are gathered in Table 1 along with their variations between the 3 groups of mice. The *p*-values of the comparisons between groups are reported in Table 2. Cumulative distributions of the concentrations of the 39 metabolites in the 3 groups of mice are presented in Figure 4; they are largely non-overlapping whenever differences between groups are significant. Differences between groups are summarized in Figure 5 that presents ratios of the mean concentrations and their 95% confidence intervals.

Significant differences are highlighted by colored symbols. These data show that *Akp2*$^{+/+}$ and *Akp2*$^{+/-}$ mice have very similar metabolomes except for cystathionine (p=0.04). In contrast, very large changes are observed for GABA, adenosine and cystathionine in knockout mice compared to *Akp2*$^{+/+}$ and *Akp2*$^{+/-}$ mice. The amplitude of the concentration variation between the TNAP-knockout mice and the other genotypes grouped together reaches ≈−40% for GABA, ≈−80% for adenosine and is much higher for cystathionine (≈ +450%) (Table 1, Figure 5).

Beyond these highly discriminating metabolites, significant differences were observed for 5 additional metabolites: methionine, 3-methylhistidine, histidine, NAA and the dipeptide N-acetyl-aspartyl-glutamate (NAAG). Although the NMR variables for these 5 metabolites were observed in the top 30 variables ranked in the VIP plots (score >1.3), other converging criteria (% variations and non-parametric tests) were taken into account for confirming the influence of TNAP in their metabolisms. The concentrations of these 5 metabolites were significantly higher in *Akp2*$^{-/-}$ than in *Akp2*$^{+/+}$ or *Akp2*$^{+/-}$ mice (Tables 1 and 2, Figures 4 and 5). Methionine and 3-methylhistidine levels were around 50% higher in TNAP-knockout mice. More modest variations (between +10 and +20%) were observed for histidine, NAA and NAAG.

Non-parametric statistical tests did not reveal any significant variations between the genotypes for the 31 other metabolites (Table 1). Although their metabolisms are associated to PLP-dependent enzymes, metabolites such as taurine, glycine, phenylalanine, pyruvate, aspartate and alanine, did not show significant variations between the 3 groups of mice.

^{31}P NMR analysis

PPi and PLP are well-established substrates of TNAP. As PLP was not detected and PPi could not be observed with our ^{1}H NMR methodology, and in an attempt to complement the analysis of phosphorylated metabolites, we performed ^{31}P NMR experiments on the same samples of brains extracts. A proton decoupled ^{31}P NMR spectrum of the aqueous extract of a wild-type (*Akp2*$^{+/+}$) mouse whole brain is presented in Figure 6. Signals were assigned by addition of authentic compounds and/or with literature data on ^{31}P NMR analysis of tissue extracts (Gribbestad *et al.* 1994; Iles *et al.* 1985). The analysis allowed the detection of PE (3.98 ppm), PC (3.46 ppm), Pi (2.74 ppm), glycerophosphocholine (−0.07 ppm), phosphocreatine (−3.08 ppm) and of the adenine nucleotides AMP (3.96 ppm, singlet), ADP (−5.75 ppm, doublet (d), $^{2}J_{PP}$ = 21.4 Hz; −10.27 ppm, d, $^{2}J_{PP}$ = 21.4 Hz) and ATP (−5.30 ppm, d, $^{2}J_{PP}$ = 17.8 Hz). The two other signals of ATP at ≈−10.5 ppm (d) and −21.4 ppm (t) were difficult to detect due to their low intensity and partial overlap with unknown signals for the doublet. Neither PPi nor PLP could be detected in the brain extracts, although addition of standard PPi and PLP revealed signals for both compounds at −5.35 ppm and 3.81 ppm respectively (not illustrated). Thus, if PPi and PLP were present, their concentrations must have been under the detection limits, which are 25 µmol/L for PLP and 12.5 µmol/L for PPi in our experimental conditions. Therefore, it appears from all these experiments that ^{31}P NMR did not add much in comparison to ^{1}H NMR.

Discussion

The aim of the present study was to specify, without any *a priori*, the products and substrates whose synthesis or use are linked, directly or indirectly, to TNAP function in the nervous tissue. As such our study was the first to use metabolomics for analyzing the brain metabolism in an animal model of HPP. We found that the levels of 8 metabolites differed between TNAP-knockout mice in comparison to wild-type and heterozygous mice. Thus, non-supervised PCA analysis indicated that the metabolome of $Akp2^{-/-}$ mice was distinct from those of $Akp2^{+/+}$ and $Akp2^{+/-}$ mice while supervised PLS-DA revealed that GABA, adenosine and cystathionine were the metabolites that most strongly distinguished $Akp2^{-/-}$ mice from the other genotypes (Figure 3). Further analyses showed that 5 other metabolites (methionine, 3-methylhistidine, histidine, NAA and NAAG) were found in significantly higher concentrations in $Akp2^{-/-}$ mice brain (Tables 1 and 2, Figures 4 and 5).

^{1}H NMR power

Untargeted ^{1}H NMR requires minimal sample preparation prior to analysis, offers relatively short analytical run times and produces highly reproducible results. It is particularly well suited to the analysis of metabolites available in limited amounts from samples of small sizes, as often occurs with brain tissue. The number of metabolites detected and quantified in our study – 39 – is in the upper range of that described in previous studies using ^{1}H NMR from brain extracts. Indeed, although Liu et al (Liu *et al.* 2013) have been able to quantify 36 metabolites in the brain of neonatal mice using a 900 MHz spectrometer, recent studies on mice brain extracts typically described less than 30 metabolites (Botosoa *et al.* 2012; Lalande *et al.* 2014; Salek *et al.* 2010). NMR analysis on human CSF is more powerful and allows the detection of >50 metabolites (Mandal *et al.* 2012; Sinclair *et al.* 2010; Smolinska *et al.* 2012; Stoop *et al.* 2010; Wishart *et al.* 2008). However, for specific diseases, it remains necessary to work in exploratory studies with animal models in which the collection of CSF is difficult to achieve. Interestingly, among the 8 metabolites highlighted in the present study, only 3 – methionine and histidine (Wishart *et al.* 2008), 3-methylhistidine (Stoop *et al.* 2010) – have been detected using untargeted ^{1}H NMR in human CSF whereas the detection of the other 5 in the CSF required alternative targeted methods – cystathionine (Strauss *et al.* 2007), adenosine (Traut 1994), GABA (Nisijima and Ishiguro 1995), NAA and NAAG (Do *et al.* 1995).

Limitations of the present study

As the ^{1}H NMR analysis was conducted on the whole brain, it is not possible to state as to whether the metabolites measured were located in the intra- or extracellular compartment and to compare metabolites levels between whole brain and CSF.

In addition, the whole brain homogenates mixed the diverse cell types that express TNAP. However TNAP vascular activity appears around 10-12 PND in the mouse brain (Fonta *et al.* 2015; Langer *et al.* 2007; Vorbrodt *et al.* 1986). Thus the metabolites affected by TNAP deficiency most likely originated from neurons and glial cells in our 7-day-old mice.

Furthermore, our ^{1}H NMR approach was limited to revealing small hydrosoluble molecules, such that there remain putative phosphoproteins and lipophilic molecules of interest that still need to be assayed for consequences of TNAP dysfunction.

Finally, we could not conclude definitely on the effect of deficient TNAP activity for a number of metabolites. Some metabolites displayed large inter-subject variability (especially nucleotides), which may have hindered detecting subtle differences between phenotypes. Furthermore, by applying a correction for multiple comparisons, our statistical analyses were quite conservative. We noticed that the cumulative distributions for some metabolites overlapped only weakly when comparing *Akp2*$^{-/-}$ mice to *Akp2*$^{+/+}$ and *Akp2*$^{+/-}$ mice, although the differences did not show up as significant (phosphocholine and betaine for example). Some of these differences might become significant in future studies on more numerous animals. Other metabolites that have been shown to be directly or indirectly related to TNAP, such as PLP, PPi and aminergic neurotransmitters, were not detected as a consequence of the relatively high detection limit of the NMR technique. Some potentially interesting metabolites such as serine, cysteine, homocysteine, alpha ketobutyrate, which could be related to cystathionine metabolism as well as to PLP-dependent enzymes, were not detected either due to their low concentrations or due to possible overlap with other metabolites.

Nevertheless we have been able to confirm reduced levels for one metabolite (GABA) (Fonta *et al.* 2012; Waymire *et al.* 1995) and to reveal, for the first time, alterations for seven other metabolites in the brain of TNAP-knockout mice.

Wild-type vs. heterozygous mice

Literature data reported that TNAP activity in the serum and different organs (bone, liver and kidney) of heterozygous transgenic mice is about 50% of that observed in wild-type mice (Fedde *et al.* 1999; Narisawa *et al.* 1997; Waymire *et al.* 1995). Despite this difference, the brain metabolomes of *Akp2*$^{+/+}$ and *Akp2*$^{+/-}$ mice appeared essentially similar, at least in 7-day- old *Apk2* mice. HPLC analyses showed that the whole brain level of PLP is very similar for the wild type and heterozygous mice (Waymire *et al.* 1995), implying that the functioning of PLP-dependent enzymes is similar in both genotypes. This is paralleled by lack of gross behavioral or phenotypic anomalies in heterozygous mice (Narisawa *et al.* 1997; Waymire *et al.* 1995).

Akp2-knockout vs. wild-type mice

Comments on the known markers of TNAP dysfunction—PE accumulates in the urine and plasma of HPP patients and of TNAP-knockout mice (Fedde *et al.* 1999; Fraser 1957; McCance *et al.* 1955). One study also reported a drastic increase of PE concentration in the CSF of young HPP patients (Balasubramaniam *et al.* 2010). Yet we did not detect any change in the whole brain of TNAP transgenic mice. The most likely reason for this discrepancy is that extracellular PE, which is amenable to dephosphorylation by TNAP, represents a tiny fraction (≤0.3%) of total PE (Hamberger and Nystrom 1984; Hamberger *et al.* 1991), such that changes in this fraction would have gone unnoticed in our whole brain-based measurements.

PPi is another classical marker of HPP. Yet, to our knowledge, no study has thus far reported PPi concentration in the normal brain and TNAP gene inactivation does not seem to be able to raise this concentration above 12.5 μM in the brain of TNAP-knockout mice.

PLP, whose concentration in whole brain extracts in rodents is of the order of 5-15 nmol/g (Masisi *et al.* 2012; Spector 1978; Waymire *et al.* 1995), was not detected with the methods we used (detection limit 25 μmol/L), such that we cannot absolutely ascertain its variation in the brain of our mouse model. Nevertheless, it is well established that extracellular PLP is primarily dephosphorylated by TNAP: studies reported markedly elevated PLP concentration in the serum of HPP patients (Whyte *et al.* 1988; Whyte *et al.* 1985). Likewise, PLP concentration appears to be elevated in the CSF of children with HPP (Belachew *et al.* 2013; Hofmann *et al.* 2013). On the other hand, Waymire *et al.* (1995) reported a 2-3 times *decrease* of PLP level in whole brain measurement in their TNAP-knockout mouse model. Since the whole brain concentration of vitamin B6 is more than ten times larger than that of the CSF (Spector 1978), the decreased PLP content reported by Waymire *et al.* (1995) must chiefly reflect a reduction in intracellular PLP content. We assume that TNAP gene ablation led to a reduction of intracellular PLP content in the *Akp2* model as well, consequently affecting the functioning of PLP-dependent enzymes. This is largely supported by the fact that most metabolites alterations reported here are also observed in vitamin B6 deficiency, as detailed below.

Metabolites related to PLP-dependent enzymes—GABA. In Waymire *et al.* (1995) mouse strain, TNAP inactivation resulted in a 50% decrease of GABA contents in 10-14 PND mice. We report here a similar decrease (≈−40%) in the *Apk2* model, confirming previous results obtained by HPLC with the same mouse strain (Fonta *et al.* 2012). This decrease can be explained by the dependence for GABA synthesis on PLP. GABA concentration is reduced in the brain of rats deprived of vitamin B6 (Guilarte 1989; Kurtz *et al.* 1972; Stephens *et al.* 1971) and is low in the brain of infants and children with vitamin B6-dependent seizures (Kurlemann *et al.* 1987; Lott *et al.* 1978).

In the mammalian brain, GABA is produced from glutamic acid by two forms of glutamate decarboxylases, GAD65 and GAD67 (Martin and Rimvall 1993), that both require PLP as cofactor. Yet GAD65 and GAD67 differ with respect to their affinities for PLP: PLP is more loosely bound to GAD65 in comparison to GAD67 (Battaglioli *et al.* 2003). This would predict that the decreased GABA level observed in vitamin B6-deprived animals and in TNAP-knockout mice was mostly due to a reduction of GAD65 activity. On the other hand, in normal brain GAD65 is mostly present in its apoenzyme form (Kaufman *et al.* 1991; Martin *et al.* 1991), such that the bulk of GABA synthesis may be ascribed to GAD67 (Mason *et al.* 2001; Patel *et al.* 2006). This is strengthened by the observation that GABA concentration is minimally altered in GAD65-knockout mice (Asada *et al.* 1996; Kash *et al.* 1997) while it is drastically reduced in GAD67-knockout mice (Asada *et al.* 1997). This would imply that the decreased GABA level observed in vitamin B6-deprived animals and in TNAP-knockout mice was mostly due to a reduction of GAD67 activity. It is to be noticed however, that GAD65 does contribute to GABA synthesis in pathological conditions, in particular epileptic seizures (Asada *et al.* 1996; Kash *et al.* 1997; Patel *et al.* 2006) that may also be observed in vitamin B6-deprived animals and in TNAP-knockout mice.

Cystathionine: Cystathionine is the intermediate compound in the two steps transsulfuration pathway that generates cysteine from homocysteine and serine. Cystathionine concentration was increased several fold in the brain of TNAP-knockout mice. Studies showed that cystathionine is the most sensitive marker of PLP deficiency in amino acid and nucleotides metabolisms (discussed in (Nijhout *et al.* 2009)). Vitamin B6 restriction in rats results in a several-fold increase of cystathionine level in the brain (Hope 1964; Kurtz *et al.* 1972; Wasynczuk *et al.* 1983). In humans with dietary vitamin B6 restriction, cystathionine level increases in blood and urine (Davis *et al.* 2006; Gregory *et al.* 2013; Lamers *et al.* 2009; Park and Linkswiler 1970). It has also been shown to accumulate in the brain of a patient with vitamin B6-dependent seizures (Lott *et al.* 1978).

Both cystathionine synthesis – by cystathionine β-synthase (CBS) – and catabolism – by cystathionine γ-lyase (CGL, also known as CSE or as cystathionase) – require PLP (e. g., (Kery *et al.* 1999; Oh and Churchich 1973; Taoka *et al.* 1999)). Yet CBS activity is less impacted than CGL by PLP deficiency (Davis *et al.* 2006; Finkelstein and Chalmers 1970; Lima *et al.* 2006; Martinez *et al.* 2000; Sato *et al.* 1996). Accumulation of cystathionine in our experimental model therefore likely resulted from the stronger dependency of CGL activity on PLP.

Expression of CGL and CBS are widely distributed in the brain (Diwakar and Ravindranath 2007; Heinonen 1973; Linden *et al.* 2008) and their developmental regulation suggests that cystathionine regulation is linked to brain development from the early embryonic to the postnatal stages (Enokido *et al.* 2005; Heinonen 1973; Robert *et al.* 2003).

To our knowledge cystathionine has not been associated to HPP or TNAP dysfunction. In other contexts, studies showed that altered tissue level of cystathionine, brain included, is reflected by increased urinary excretion of cystathionine (Espinos *et al.* 2010; Harris *et al.* 1959; Hope 1957; 1964; Kraus *et al.* 2009). This opens the possibility of using cystathionine as an additional marker for diagnostic purposes in HPP.

Methionine: Methionine is metabolically linked to cystathionine through the methionine cycle and the transsulfuration pathway. In normal conditions, the two pathways share a common substrate, which is homocysteine: homocysteine can either be transformed in cystathionine through the action of CBS (first step of the transsulfuration pathway), or can be used to synthetize methionine through methylation. Methionine is then converted back to homocysteine through a two-step-process (methionine cycle). Accumulation of methionine (+50%) in the TNAP-knockout mouse brain may be the consequence of the increased amount of cystathionine that may result in an accumulation of homocysteine that would in turn be diverted to form additional methionine. In support of this possibility, studies showed that not only cystathionine, but also homocysteine and methionine are present in higher concentrations in the blood of CGL-knockout than in wild-type mice (Ishii *et al.* 2010; Jiang *et al.* 2015; Yang *et al.* 2008). Methionine accumulation would therefore be an indirect consequence of PLP deficiency.

Histidine: Histidine accumulated in the brains of our TNAP deficient mice (+20%). Histidine is a precursor for histamine through PLP-dependent histidine decarboxylase

(HDC) (Kahlson and Rosengren 1968; Watanabe *et al.* 1991). Thus accumulation of histidine may be readily explained by reduced availability of intracellular PLP. We hypothesize that increased levels of histidine in TNAP-knockout mice could lead to lower level of histamine, a multipotent compound that is devoted to homeostatic (biological rhythms, thermoregulation, stress) and higher (mood, cognition, learning and memory) brain functions and that may also regulate brain development (Karlstedt *et al.* 2003; Karlstedt *et al.* 2001; Kinnunen *et al.* 1998). Alteration of histamine level in TNAP-knockout mice could precipitate the effects produced by the dysregulation of other metabolites. Further HPLC analyses would help to establish a link between histidine accumulation and altered histaminergic system in hypophosphatasia, which has not been reported till now.

3-Methylhistidine: Schwartz and colleagues (Schwartz *et al.* 1973) suggested that methylhistidine could be another substrate of the HDC. Thus, as for histidine, 3-methylhistidine accumulation in the brain of TNAP-knockout mice might result from reduction of intracellular PLP. Although it is mostly known as a constituent of the myofibrillar proteins actin and myosin (Elzinga *et al.* 1973; Long *et al.* 1988; Long *et al.* 1975; Young *et al.* 1972), 3-methylhistidine has also been detected in the CSF (Ferraro and Hare 1985; Gerrits *et al.* 1998; Stoop *et al.* 2010). The functions of 3-methylhistidine in the brain and the consequences of its accumulation are not, to our knowledge, established.

Adenosine—We found that the adenosine level was dramatically reduced (≈−80%) in the brain of TNAP-knockout mice. There are several possible explanations for this reduction. One first possibility is related to the ectonucleotidase activity of TNAP, and in particular its ability to dephosphorylate AMP to adenosine, that has been documented for various tissues (e.g., (Ciancaglini *et al.* 2010; Picher *et al.* 2003; Say *et al.* 1991; van Belle 1976)). This activity has also been reported in brain homogenates (Dorai and Bachhawat 1977), in brain cell cultures (Diez-Zaera *et al.* 2011; Ohkubo *et al.* 2000) and in the spinal cord *in vitro* (Street *et al.* 2013). If the decreased adenosine concentration we observed resulted from a compromised ectonucleotidase activity, it should have been associated with an increase in adenine nucleotide levels, which we did not detect (Fig. 5). It is to be noticed however that adenosine level represents a minute fraction of the sum of adenosine and adenine nucleotide levels: 2.3% in $Akp2^{+/+}$ and 0.3% in $Akp2^{-/-}$ mice. This implies that the total adenine nucleotide level should increase by ≈2% in *Akp2*-knockout mice. Yet such a small increase would go unnoticed given the large intersubject variability (for purpose of comparison the 95% confidence intervals for ATP, ADP and AMP in *Akp2* mice represented between 7% and 36% of the means).

TNAP is not the sole nucleotidase that can generate adenosine. Extracellular adenosine results from the successive dephosphorylation of ATP released in the extracellular space in ADP and AMP by several ectonucleotidases (e.g., (Zimmermann *et al.* 2012)) among which TNAP is the only one capable to ensure all the dephosphorylation steps of the adenosine nucleotides. Apart from TNAP, ecto-5′-nucleotidase ensures extracellular AMP to adenosine conversion in the brain. In the cytoplasm adenosine is also produced from AMP by cytosolic-5′-nucleotidase I (Le *et al.* 2014; Sala-Newby *et al.* 1999).

The effect of TNAP dysfunction on adenosine level in our 7-day-old mice is much larger than what could be anticipated from studies performed in older rodents (e.g. (Kulesskaya *et al.* 2013; Lovatt *et al.* 2012; Street *et al.* 2013; Wall and Dale 2013; Zhang *et al.* 2012)). In those studies, the contribution of TNAP to extracellular adenosine synthesis appears to be minor in comparison to that of ecto-5′-nucleotidase. A possible explanation for this discrepancy resides in opposite developmental changes for TNAP and 5′-nucleotidase activities: TNAP is most strongly expressed in embryos and in early postnatal ages, and its expression thereafter declines during postnatal development (Goldstein and Harris 1981; Langer *et al.* 2007; Narisawa *et al.* 1994); on the contrary both cytosolic- and ecto-5′-nucleotidase expression/activity progressively increase during postnatal development (Grkovic *et al.* 2014; Mackiewicz *et al.* 2006).

Another possibility for explaining reduced adenosine level in TNAP-knockout mice, quite relevant in the context of the present study, pertains to the methionine cycle and the transsulfuration pathway. In the methionine cycle, homocysteine is methylated to yield methionine. The methionine cycle continues with the production of S-adenosylmethionine, which in turn can be demethylated to produce S-adenosylhomocysteine (SAH). SAH hydrolase completes the loop by regenerating homocysteine and by generating adenosine. Therefore, under normal conditions the methionine cycle is another source of adenosine. Interestingly, in liver and thymus of vitamin B6-deprived animals, accumulation of cystathionine is reverberated by an increase in homocysteine, which results in an increase of SAH (Isa *et al.* 2006; Nguyen *et al.* 2001). This was explained by a reversal of SAH hydrolase activity (Isa *et al.* 2006); in vitamin B6 deficiency therefore, SAH hydrolase should not produce, but should instead consume adenosine. Likewise, the reduction of intracellular PLP in TNAP-knockout mice could lead to a decrease of intracellular adenosine. Unfortunately the only study we are aware of (Nguyen *et al.* 2001), that examined consequences of vitamin B6 deficiency on SAH concentration in the brain, found no difference in comparison to normally fed controls, although it reported strong increase in SAH level in liver and thymus. However, this result was obtained in 9-week-old rats and may not be transposed to our 7-day-old mice.

N-Acetylaspartate / N-acetyl-aspartyl-glutamate—NAA and NAAG, whose biosynthesis is covered by enzymes that are *not* PLP-dependent, tended to accumulate (around +15-20%) in mice whose TNAP gene had been inactivated. NAAG is synthesized from NAA at constant rate and both metabolites are catabolized at the same rate, such that their concentrations are maintained at a constant ratio (Baslow *et al.* 2007). This may explain the higher level of NAAG that would simply follow NAA accumulation. NAA is produced in neurons and is taken up by oligodendrocytes, where it is split into aspartate and acetyl-CoA by aspartoacylase. Acetyl-CoA is involved in the metabolism of fatty acids and is incorporated in lipids required for myelin lipid synthesis (Chakraborty *et al.* 2001; Namboodiri *et al.* 2006). In TNAP-knockout mice, compromised myelination (Hanics *et al.* 2012) could result in less fatty acids demand for myelin formation. Therefore, NAA would not be converted and would accumulate instead.

This hypothesis is supported by results obtained in aspartoacylase-knockout mice (Matalon *et al.* 2000; Nordengen *et al.* 2015) and in Cavanan disease, which is caused by a deficiency

of aspartoacylase activity (Hagenfeldt *et al.* 1987; Hoshino and Kubota 2014; Wolf *et al.* 2004): in both cases, hypomyelination and white matter degeneration are associated with high levels of NAA in the urine, CSF and brain tissue.

Phenotypic features of HPP in relation to brain metabolome changes

The severe forms of HPP often present with seizures, apnea, deafness and encephalopathy (Hofmann *et al.* 2013; Taketani 2015). These disorders were initially considered to be consequences of deficient TNAP activity in other tissues, especially bone tissue in which TNAP plays an essential role in mineralization. For example, epilepsy and apnea were explained by cranial deformities and reduced thoracic volume by insufficient mineralization of the ribs. However other clinical (Baumgartner-Sigl *et al.* 2007; Belachew *et al.* 2013; Bethenod *et al.* 1967; de Roo *et al.* 2014; Taketani *et al.* 2014) data evidenced that neurological consequences of TNAP gene deficits can be dissociated from bone defects. Moreover experimental data (Foster *et al.* 2016) do not report any neurological disorders in mice in which TNAP deletion specifically targets bone and tooth cells, supporting the hypothesis that the neurological disorders observed in the severe form of hypophosphatasia are directly caused by TNAP dysfunction in the brain rather than indirectly in other tissues.

One of the main feature of perinatal and, to a lesser degree, infantile HPP, is the occurrence of epileptic seizures (e. g. (Bethenod *et al.* 1967; Fraser 1957; Rathbun 1948; Whyte *et al.* 1988)), which are also observed in TNAP-knockout mice (Narisawa *et al.* 1997; Narisawa *et al.* 2001; Waymire *et al.* 1995). Seizures are classically attributed to defective GABAergic inhibition (reviewed in (Cossart *et al.* 2005; Macdonald *et al.* 2010)). Given that GABA is synthesized by PLP-dependent enzymes (see above) and since PLP metabolism appears defective in HPP, it quite logically follows that epileptic seizures in HPP patients and TNAP-knockout mice should result from defective GABAergic inhibition. Accordingly seizures observed in HPP patients may be controlled with vitamin B6 (Balasubramaniam *et al.* 2010; Baumgartner-Sigl *et al.* 2007; Belachew *et al.* 2013; de Roo *et al.* 2014; Demirbilek *et al.* 2012; Litmanovitz *et al.* 2002; Nakamura-Utsunomiya *et al.* 2010; Nunes *et al.* 2002; Sia *et al.* 1975; Yamamoto *et al.* 2004). Yet this treatment is not always successful (Bethenod *et al.* 1967; Hofmann *et al.* 2013; Posen *et al.* 1997) or the improvement may be only transitory (de Roo *et al.* 2014; Nakamura-Utsunomiya *et al.* 2010; Whyte *et al.* 1988). Despite vitamin B6 treatment, seizures also recur in *Akp2*-knockout mice (Narisawa *et al.* 2001). This suggests that in addition to GABA, TNAP dysfunction has consequences on other metabolites that may play a role in controlling epileptic seizures. One of these metabolites is adenosine.

Extracellular adenosine influences neuronal activity through two types of receptors, which reduce excitatory synaptic transmission (A1 receptors) or modulate inhibitory synaptic transmission (A2 receptors) (for review: (Cunha 2001; Rodrigues *et al.* 2015)). Blocking adenosine receptors results in a worsening and a prolongation of seizures induced by other means whereas adenosine and adenosine receptor agonists display anti-convulsive properties (Boison 2012; Dragunow *et al.* 1985; Maitre *et al.* 1974; Pagonopoulou *et al.* 2006). The dramatic reduction of adenosine level in TNAP-knockout mice implies that one natural means of controlling seizures is also deficient.

Among other alterations, myelination appears defective in TNAP-knockout mice (Hanics *et al.* 2012; Narisawa *et al.* 1997) while white matter appears abnormal in HPP patients (de Roo *et al.* 2014; Hofmann *et al.* 2013; Nunes *et al.* 2002). TNAP may intervene in myelination through both nucleotide and PLP metabolisms. First, the earliest stage of myelination is promoted by extracellular adenosine (Stevens *et al.* 2002). Later stages depend on the extracellular concentration of ATP (Ishibashi *et al.* 2006). Thus TNAP gene inactivation and subsequent decrease in adenosine level may compromise myelination. We recently speculated that levamisole-induced multifocal leukoencephalopathy is based on the same mechanisms (Nowak *et al.* 2015). Secondly, myelination is altered in vitamin B6 deficiency (Jardim *et al.* 1994; Lott *et al.* 1978; Morre *et al.* 1978). This is paralleled by decreases in the amount of sphingolipids in the brain of rats deprived of vitamin B6 (Kurtz *et al.* 1972; Stephens and Dakshinamurti 1975). Sphingomyelin synthesis involves two PLP-dependent enzymes (Bourquin *et al.* 2011). Although lipophilic metabolites were not examined in our study, accumulation of NAA and NAAG suggests that the metabolism of fatty acids was indeed altered in our TNAP-knockout mice.

Our study revealed dysregulation of the methionine cycle and transsulfuration pathway in the brain of TNAP-knockout mice, evidenced by a significant increase in methionine level and by a several fold increase in cystathionine concentration. The roles of cystathionine in neuronal development have not been examined and studies exploring its neural functions were not conclusive (Key and White 1970; Regnier *et al.* 2012; Werman *et al.* 1966). It is worth mentioning that patients with CGL mutations may express neurologic symptoms such as seizures and mental retardation (Espinos *et al.* 2010; Frimpter 1965; Kraus *et al.* 2009). This suggests that alteration of cystathionine level or, more generally, of the transsulfuration pathway from methionine to cysteine, glutathione and hydrogen sulfide, may also contribute to the neurologic defects observed in HPP. This possibility warrants further study.

Acknowledgments

The authors wish to acknowledge Hypophosphatasie Europe for financial support (ref CNRS n° 088461). They thank Fabrice Collin and Catherine Claparols for mass spectrometry experiments and Camille Grange for his contribution to the animal care and breeding.

List of abbreviations

Ace	acetate
Ade	adenine
Ala	alanine
AP	alkaline phosphatase
Asn	asparagine
Asp	aspartate
AXP	adenosine mono-, di- and triphosphate
Bet	betaine

CBS	cystathionine β-synthase
CGL	cystathionine γ-lyase
Cho	choline
CI	confidence interval
Cit	citrate
Cr	creatine
CXP	cytidine mono-, di- and triphosphate
FID	free induction decay
Fum	fumarate
GAD	glutamate decarboxylase
GDP	guanosine diphosphate
Gln	glutamine
Glu	glutamate
Gly	glycine
GMP	guanosine monophosphate
GPC	glycerophosphocholine
GTP	guanosine triphosphate
GXP	guanosine mono-, di- and triphosphate
His	histidine
HPP	hypophosphatasia
Ile	isoleucine
Lac	lactate
Leu	leucine
Mal	malate
MeOH	methanol
3-MHis	3-methylhistidine
MS	mass spectrometry
NAA	N-acetylaspartate
NAAG	N-acetyl-aspartyl-glutamate

Nico	nicotinamide
Oxo	oxoproline
PC	phosphocholine
PCA	principal component analysis
PCr	phosphocreatine
PE	phosphoethanolamine
Phe	phenylalanine
PL	pyridoxal
PLP	pyridoxal phosphate
PLS-DA	Partial Least Squares Discriminant Analysis
PND	postnatal day
ppm	parts per million
SAH	S-adenosylhomocysteine
S/N	signal-to-noise ratio
SRM	selected reaction monitoring
Suc	succinate
Tau	taurine
TNAP	Tissue Nonspecific Alkaline Phosphatase
Trp	tryptophan
TSP	Sodium 2,2,3,3-tetradeutero-3-trimethylsilylpropionate
Tyr	tyrosine
UDP	uridine diphosphate
UMP	uridine monophosphate
UHPLC	ultra-high performance liquid chromatography
UTP	uridine triphosphate
UXP	uridine mono-, di- and triphosphate
Val	valine
VIP	variable importance in the projection

References

Anstrom JA, Brown WR, Moody DM, Thore CR, Challa VR, Block SM. Anatomical analysis of the developing cerebral vasculature in premature neonates: absence of precapillary arteriole-to-venous shunts. Pediatr. Res. 2002; 52:554–560. [PubMed: 12357050]

Asada H, Kawamura Y, Maruyama K, et al. Mice lacking the 65 kDa isoform of glutamic acid decarboxylase (GAD65) maintain normal levels of GAD67 and GABA in their brains but are susceptible to seizures. Biochem. Biophys. Res. Commun. 1996; 229:891–895. [PubMed: 8954991]

Asada H, Kawamura Y, Maruyama K, et al. Cleft palate and decreased brain gamma-aminobutyric acid in mice lacking the 67-kDa isoform of glutamic acid decarboxylase. Proceedings of the National Academy of Sciences of the United States of America. 1997; 94:6496–6499. [PubMed: 9177246]

Balasubramaniam S, Bowling F, Carpenter K, Earl J, Chaitow J, Pitt J, Mornet E, Sillence D, Ellaway C. Perinatal hypophosphatasia presenting as neonatal epileptic encephalopathy with abnormal neurotransmitter metabolism secondary to reduced cofactor pyridoxal-5′-phosphate availability. J. Inherit. Metab. Dis. 2010; (Suppl 3):S25–S33. [PubMed: 20049532]

Balayssac S, Déjean S, Lalande J, Gilard V, Malet-Martino M. A toolbox to explore NMR metabolomic data sets using the R environment. Chemometrics and Intelligent Laboratory Systems. 2013; 126:50–59.

Bartl J, Chrastina P, Krijt J, Hodik J, Peskova K, Kozich V. Simultaneous determination of cystathionine, total homocysteine, and methionine in dried blood spots by liquid chromatography/tandem mass spectrometry and its utility for the management of patients with homocystinuria. Clin. Chim. Acta. 2014; 437:211–217. [PubMed: 25086281]

Baslow MH, Hrabe J, Guilfoyle DN. Dynamic relationship between neurostimulation and N-acetylaspartate metabolism in the human visual cortex: evidence that NAA functions as a molecular water pump during visual stimulation. J. Mol. Neurosci. 2007; 32:235–245. [PubMed: 17873369]

Battaglioli G, Liu H, Martin DL. Kinetic differences between the isoforms of glutamate decarboxylase: implications for the regulation of GABA synthesis. J. Neurochem. 2003; 86:879–887. [PubMed: 12887686]

Baumgartner-Sigl S, Haberlandt E, Mumm S, Scholl-Burgi S, Sergi C, Ryan L, Ericson KL, Whyte MP, Hogler W. Pyridoxine-responsive seizures as the first symptom of infantile hypophosphatasia caused by two novel missense mutations (c.677T>C, p.M226T; c.1112C>T, p.T371I) of the tissue-nonspecific alkaline phosphatase gene. Bone. 2007; 40:1655–1661. [PubMed: 17395561]

Beckonert O, Keun HC, Ebbels TM, Bundy J, Holmes E, Lindon JC, Nicholson JK. Metabolic profiling, metabolomic and metabonomic procedures for NMR spectroscopy of urine, plasma, serum and tissue extracts. Nat Protoc. 2007; 2:2692–2703. [PubMed: 18007604]

Belachew D, Kazmerski T, Libman I, Goldstein AC, Stevens ST, Deward S, Vockley J, Sperling MA, Balest AL. Infantile hypophosphatasia secondary to a novel compound heterozygous mutation presenting with pyridoxine-responsive seizures. JIMD reports. 2013; 11:17–24. [PubMed: 23479201]

Bell MA, Ball MJ. Laminar variation in the microvascular architecture of normal human visual cortex (area 17). Brain research. 1985; 335:139–143. [PubMed: 4005537]

Bethenod M, Cotte MF, Collombel C, Frederich A, Cotte J. [Neonatal discovery of hypophosphatasia. Bone improvement. Fatal convulsant encephalopathy]. Ann. Pediatr. (Paris). 1967; 14:835–841. [PubMed: 4299440]

Boison D. Adenosine dysfunction in epilepsy. Glia. 2012; 60:1234–1243. [PubMed: 22700220]

Botosoa EP, Zhu M, Marbeuf-Gueye C, Triba MN, Dutheil F, Duyckaerts C, Beaune P, Loriot MA, Le Moyec L. NMR metabolomic of frontal cortex extracts: First study comparing two neurodegenerative diseases, Alzheimer disease and amyotrophic lateral sclerosis. Irbm. 2012; 33:281–286.

Bourquin F, Capitani G, Grutter MG. PLP-dependent enzymes as entry and exit gates of sphingolipid metabolism. Protein Sci. 2011; 20:1492–1508. [PubMed: 21710479]

Brun-Heath I, Ermonval M, Chabrol E, et al. Differential expression of the bone and the liver tissue non-specific alkaline phosphatase isoforms in brain tissues. Cell Tissue Res. 2011; 343:521–536. [PubMed: 21191615]

Buchet R, Millan JL, Magne D. Multisystemic functions of alkaline phosphatases. Methods Mol. Biol. 2013; 1053:27–51. [PubMed: 23860646]

Chakraborty G, Mekala P, Yahya D, Wu G, Ledeen RW. Intraneuronal N-acetylaspartate supplies acetyl groups for myelin lipid synthesis: evidence for myelin-associated aspartoacylase. J. Neurochem. 2001; 78:736–745. [PubMed: 11520894]

Ciancaglini P, Yadav MC, Simao AM, Narisawa S, Pizauro JM, Farquharson C, Hoylaerts MF, Millan JL. Kinetic analysis of substrate utilization by native and TNAP-, NPP1-, or PHOSPHO1-deficient matrix vesicles. J. Bone Miner. Res. 2010; 25:716–723. [PubMed: 19874193]

Coburn SP. Vitamin B-6 Metabolism and Interactions with TNAP. Subcell. Biochem. 2015; 76:207–238. [PubMed: 26219714]

Cossart R, Bernard C, Ben-Ari Y. Multiple facets of GABAergic neurons and synapses: multiple fates of GABA signalling in epilepsies. Trends in neurosciences. 2005; 28:108–115. [PubMed: 15667934]

Cunha RA. Adenosine as a neuromodulator and as a homeostatic regulator in the nervous system: different roles, different sources and different receptors. Neurochem. Int. 2001; 38:107–125. [PubMed: 11137880]

Davis SR, Quinlivan EP, Stacpoole PW, Gregory JF 3rd. Plasma glutathione and cystathionine concentrations are elevated but cysteine flux is unchanged by dietary vitamin B-6 restriction in young men and women. J. Nutr. 2006; 136:373–378. [PubMed: 16424114]

Daw MI, Ashby MC, Isaac JT. Coordinated developmental recruitment of latent fast spiking interneurons in layer IV barrel cortex. Nature neuroscience. 2007; 10:453–461. [PubMed: 17351636]

de Roo MG, Abeling NG, Majoie CB, Bosch AM, Koelman JH, Cobben JM, Duran M, Poll-The BT. Infantile hypophosphatasia without bone deformities presenting with severe pyridoxine-resistant seizures. Mol. Genet. Metab. 2014; 111:404–407. [PubMed: 24100244]

Demirbilek H, Alanay Y, Alikasifoglu A, Topcu M, Mornet E, Gonc N, Ozon A, Kandemir N. Hypophosphatasia presenting with pyridoxine-responsive seizures, hypercalcemia, and pseudotumor cerebri: case report. Journal of clinical research in pediatric endocrinology. 2012; 4:34–38. [PubMed: 22394703]

Diez-Zaera M, Diaz-Hernandez JI, Hernandez-Alvarez E, Zimmermann H, Diaz-Hernandez M, Miras-Portugal MT. Tissue-nonspecific alkaline phosphatase promotes axonal growth of hippocampal neurons. Mol. Biol. Cell. 2011; 22:1014–1024. [PubMed: 21289095]

Diwakar L, Ravindranath V. Inhibition of cystathionine-gamma-lyase leads to loss of glutathione and aggravation of mitochondrial dysfunction mediated by excitatory amino acid in the CNS. Neurochem. Int. 2007; 50:418–426. [PubMed: 17095121]

Do KQ, Lauer CJ, Schreiber W, Zollinger M, Gutteckamsler U, Cuenod M, Holsboer F. Gamma-Glutamylglutamine and Taurine Concentrations Are Decreased in the Cerebrospinal-Fluid of Drug-Naive Patients with Schizophrenic Disorders. J. Neurochem. 1995; 65:2652–2662. [PubMed: 7595563]

Dorai DT, Bachhawat BK. Purification and properties of brain alkaline phosphatase. J. Neurochem. 1977; 29:503–512. [PubMed: 19566]

Dragunow M, Goddard GV, Laverty R. Is adenosine an endogenous anticonvulsant? Epilepsia. 1985; 26:480–487. [PubMed: 4043018]

Dumas ME, Davidovic L. Metabolic Profiling and Phenotyping of Central Nervous System Diseases: Metabolites Bring Insights into Brain Dysfunctions. Journal of neuroimmune pharmacology : the official journal of the Society on NeuroImmune Pharmacology. 2015; 10:402–424. [PubMed: 25616565]

Elzinga M, Collins JH, Kuehl WM, Adelstein RS. Complete amino-acid sequence of actin of rabbit skeletal muscle. Proceedings of the National Academy of Sciences of the United States of America. 1973; 70:2687–2691. [PubMed: 4517681]

Enokido Y, Suzuki E, Iwasawa K, Namekata K, Okazawa H, Kimura H. Cystathionine beta-synthase, a key enzyme for homocysteine metabolism, is preferentially expressed in the radial glia/astrocyte lineage of developing mouse CNS. FASEB J. 2005; 19:1854–1856. [PubMed: 16160063]

Ermonval M, Baudry A, Baychelier F, et al. The cellular prion protein interacts with the tissue non-specific alkaline phosphatase in membrane microdomains of bioaminergic neuronal cells. PloS one. 2009; 4:e6497. [PubMed: 19652718]

Espinos C, Garcia-Cazorla A, Martinez-Rubio D, Martinez-Martinez E, Vilaseca MA, Perez-Duenas B, Kozich V, Palau F, Artuch R. Ancient origin of the CTH alelle carrying the c.200C>T (p.T67I) variant in patients with cystathioninuria. Clin. Genet. 2010; 78:554–559. [PubMed: 20584029]

Fedde KN, Blair L, Silverstein J, et al. Alkaline phosphatase knock-out mice recapitulate the metabolic and skeletal defects of infantile hypophosphatasia. J. Bone Miner. Res. 1999; 14:2015–2026. [PubMed: 10620060]

Fedde KN, Whyte MP. Alkaline phosphatase (tissue-nonspecific isoenzyme) is a phosphoethanolamine and pyridoxal-5′-phosphate ectophosphatase: normal and hypophosphatasia fibroblast study. Am. J. Hum. Genet. 1990; 47:767–775. [PubMed: 2220817]

Ferraro TN, Hare TA. Free and conjugated amino acids in human CSF: influence of age and sex. Brain research. 1985; 338:53–60. [PubMed: 4027591]

Finkelstein JD, Chalmers FT. Pyridoxine effects on cystathionine synthase in rat liver. J. Nutr. 1970; 100:467–469. [PubMed: 5439354]

Fonta C, Barone P, Rodriguez Martinez L. Negyessy L. Rediscovering TNAP in the Brain: A Major Role in Regulating the Function and Development of the Cerebral Cortex. Subcell. Biochem. 2015; 76:85–106. [PubMed: 26219708]

Fonta C, Imbert M. Vascularization in the primate visual cortex during development. Cereb Cortex. 2002; 12:199–211. [PubMed: 11739267]

Fonta C, Negyessy L, Brun Heath I, Ermonval M, Czege D, Nowak L, Frances B, Xiao J, Millan J. TNAP in the brain: functions in neurotransmission. Bull. Group. Int. Rech. Sci. Stomatol. Odontol. 2012; 51:e27.

Fonta C, Negyessy L, Renaud L, Barone P. Areal and subcellular localization of the ubiquitous alkaline phosphatase in the primate cerebral cortex: evidence for a role in neurotransmission. Cereb Cortex. 2004; 14:595–609. [PubMed: 15054075]

Fonta C, Negyessy L, Renaud L, Barone P. Postnatal development of alkaline phosphatase activity correlates with the maturation of neurotransmission in the cerebral cortex. J. Comp. Neurol. 2005; 486:179–196. [PubMed: 15844208]

Foster BL, Kuss P, Yadav MC, et al. Conditional Alpl Ablation Phenocopies Dental Defects of Hypophosphatasia. J. Dent. Res. 2016; doi: 10.1177/0022034516663633

Franz, VH. Ratios: A short guide to confidence limits and proper use. 2007. arXiv:0710.2024 [stat.AP]

Fraser D. Hypophosphatasia. Am. J. Med. 1957; 22:730–746. [PubMed: 13410963]

Fraser D, Yendt ER, Christie FH. Metabolic abnormalities in hypophosphatasia. Lancet. 1955; 268:286.

Friede RL. A quantitative mapping of alkaline phosphatase in the brain of the rhesus monkey. J. Neurochem. 1966; 13:197–203. [PubMed: 4957290]

Frimpter GW. Cystathioninuria: nature of the defect. Science. 1965; 149:1095–1096. [PubMed: 5826521]

Gerrits GP, Kamphuis S, Monnens LA, Trijbels JM, Schroder CH, Koster A, Gabreels FJ. Cerebrospinal fluid levels of amino acids in infants and young children with chronic renal failure. Neuropediatrics. 1998; 29:35–39. [PubMed: 9553947]

Goldstein DJ, Harris H. Mammalian brain alkaline phosphatase: expression of liver/bone/kidney locus. Comparison of fetal and adult activities. J. Neurochem. 1981; 36:53–57. [PubMed: 7193242]

Gonzalez-Riano C, Garcia A, Barbas C. Metabolomics studies in brain tissue: A review. J. Pharm. Biomed. Anal. 2016; 130:141–168. [PubMed: 27451335]

Greenberg CR, Taylor CL, Haworth JC, Seargeant LE, Philipps S, Triggs-Raine B, Chodirker BN. A homoallelic Gly317-->Asp mutation in ALPL causes the perinatal (lethal) form of hypophosphatasia in Canadian mennonites. Genomics. 1993; 17:215–217. [PubMed: 8406453]

Gregory JF 3rd, Park Y, Lamers Y, et al. Metabolomic analysis reveals extended metabolic consequences of marginal vitamin B-6 deficiency in healthy human subjects. PloS one. 2013; 8:e63544. [PubMed: 23776431]

Gribbestad IS, Petersen SB, Fjosne HE, Kvinnsland S, Krane J. 1H NMR spectroscopic characterization of perchloric acid extracts from breast carcinomas and non-involved breast tissue. NMR Biomed. 1994; 7:181–194. [PubMed: 7946996]

Grkovic I, Bjelobaba I, Nedeljkovic N, Mitrovic N, Drakulic D, Stanojlovic M, Horvat A. Developmental increase in ecto-5′-nucleotidase activity overlaps with appearance of two immunologically distinct enzyme isoforms in rat hippocampal synaptic plasma membranes. J. Mol. Neurosci. 2014; 54:109–118. [PubMed: 24563227]

Guilarte TR. Regional changes in the concentrations of glutamate, glycine, taurine, and GABA in the vitamin B-6 deficient developing rat brain: association with neonatal seizures. Neurochem. Res. 1989; 14:889–897. [PubMed: 2574423]

Hagenfeldt, L., Bollgren I., Venizelos, N. N-acetylaspartic aciduria due to aspartoacylase deficiency--a new aetiology of childhood leukodystrophy. J. Inherit. Metab. Dis. 1987; 10:135–141. [PubMed: 3116332]

Hamberger A, Nystrom B. Extra- and intracellular amino acids in the hippocampus during development of hepatic encephalopathy. Neurochem. Res. 1984; 9:1181–1192. [PubMed: 6504234]

Hamberger A, Nystrom B, Larsson S, Silfvenius H, Nordborg C. Amino acids in the neuronal microenvironment of focal human epileptic lesions. Epilepsy Res. 1991; 9:32–43. [PubMed: 1909237]

Hanics J, Barna J, Xiao J, Millan JL, Fonta C, Negyessy L. Ablation of TNAP function compromises myelination and synaptogenesis in the mouse brain. Cell Tissue Res. 2012; 349:459–471. [PubMed: 22696173]

Harmey D, Hessle L, Narisawa S, Johnson KA, Terkeltaub R, Millan JL. Concerted regulation of inorganic pyrophosphate and osteopontin by akp2, enpp1, and ank: an integrated model of the pathogenesis of mineralization disorders. Am J Pathol. 2004; 164:1199–1209. [PubMed: 15039209]

Harris H, Penrose LS, Thomas DH. Cystathioniuria. Ann. Hum. Genet. 1959; 23:442–453. [PubMed: 14399948]

Heinonen K. Studies on cystathionase activity in rat liver and brain during development. Effects of hormones and amino acids in vivo. Biochem. J. 1973; 136:1011–1015. [PubMed: 4786524]

Hofmann C, Liese J, Schwarz T, et al. Compound heterozygosity of two functional null mutations in the ALPL gene associated with deleterious neurological outcome in an infant with hypophosphatasia. Bone. 2013; 55:150–157. [PubMed: 23454488]

Hope DB. L-cystathionine in the urine of pyridoxine-deficient rats. Biochem. J. 1957; 66:486–489. [PubMed: 13459885]

Hope DB. Cystathionine Accumulation in the Brains of Pyridoxine-Deficient Rats. J. Neurochem. 1964; 11:327–332. [PubMed: 14165979]

Hoshi K, Amizuka N, Oda K, Ikehara Y, Ozawa H. Immunolocalization of tissue non-specific alkaline phosphatase in mice. Histochem. Cell Biol. 1997; 107:183–191. [PubMed: 9105889]

Hoshino H, Kubota M. Canavan disease: clinical features and recent advances in research. Pediatr. Int. 2014; 56:477–483. [PubMed: 24977939]

Huguet F, Guerraoui A, Barrier L, Guilloteau D, Tallineau C, Chalon S. Changes in excitatory amino acid levels and tissue energy metabolites of neonate rat brain after hypoxia and hypoxia-ischemia. Neurosci. Lett. 1998; 240:102–106. [PubMed: 9486482]

Iles RA, Stevens AN, Griffiths JR, Morris PG. Phosphorylation status of liver by 31P-n.m.r. spectroscopy, and its implications for metabolic control. A comparison of 31P-n.m.r. spectroscopy (in vivo and in vitro) with chemical and enzymic determinations of ATP, ADP and Pi. Biochem. J. 1985; 229:141–151.

Isa Y, Tsuge H, Hayakawa T. Effect of vitamin B6 deficiency on S-adenosylhomocysteine hydrolase activity as a target point for methionine metabolic regulation. J. Nutr. Sci. Vitaminol. (Tokyo). 2006; 52:302–306. [PubMed: 17190099]

Ishibashi T, Dakin KA, Stevens B, Lee PR, Kozlov SV, Stewart CL, Fields RD. Astrocytes promote myelination in response to electrical impulses. Neuron. 2006; 49:823–832. [PubMed: 16543131]

Ishii I, Akahoshi N, Yamada H, Nakano S, Izumi T, Suematsu M. Cystathionine gamma-Lyase-deficient mice require dietary cysteine to protect against acute lethal myopathy and oxidative injury. The Journal of biological chemistry. 2010; 285:26358–26368. [PubMed: 20566639]

Jardim LB, Pires RF, Martins CE, Vargas CR, Vizioli J, Kliemann FA, Giugliani R. Pyridoxine-dependent seizures associated with white matter abnormalities. Neuropediatrics. 1994; 25:259–261. [PubMed: 7885536]

Jiang H, Hurt KJ, Breen K, Stabler SP, Allen RH, Orlicky DJ, Maclean KN. Sex-specific dysregulation of cysteine oxidation and the methionine and folate cycles in female cystathionine gamma-lyase null mice: a serendipitous model of the methylfolate trap. Biology open. 2015; 4:1154–1162. [PubMed: 26276101]

Kahlson G, Rosengren E. New approaches to the physiology of histamine. Physiol. Rev. 1968; 48:155–196. [PubMed: 4169682]

Kantor O, Cserpan D, Volgyi B, Lukats A, Somogyvari Z. The Retinal TNAP. Subcell. Biochem. 2015; 76:107–123. [PubMed: 26219709]

Karlstedt K, Ahman MJ, Anichtchik OV, Soinila S, Panula P. Expression of the H3 receptor in the developing CNS and brown fat suggests novel roles for histamine. Mol. Cell. Neurosci. 2003; 24:614–622. [PubMed: 14664812]

Karlstedt K, Nissinen M, Michelsen KA, Panula P. Multiple sites of L-histidine decarboxylase expression in mouse suggest novel developmental functions for histamine. Dev. Dyn. 2001; 221:81–91. [PubMed: 11357196]

Kash SF, Johnson RS, Tecott LH, Noebels JL, Mayfield RD, Hanahan D, Baekkeskov S. Epilepsy in mice deficient in the 65-kDa isoform of glutamic acid decarboxylase. Proceedings of the National Academy of Sciences of the United States of America. 1997; 94:14060–14065. [PubMed: 9391152]

Kaufman DL, Houser CR, Tobin AJ. Two forms of the gamma-aminobutyric acid synthetic enzyme glutamate decarboxylase have distinct intraneuronal distributions and cofactor interactions. J. Neurochem. 1991; 56:720–723. [PubMed: 1988566]

Kermer V, Ritter M, Albuquerque B, Leib C, Stanke M, Zimmermann H. Knockdown of tissue nonspecific alkaline phosphatase impairs neural stem cell proliferation and differentiation. Neurosci. Lett. 2010; 485:208–211. [PubMed: 20849921]

Kery V, Poneleit L, Meyer JD, Manning MC, Kraus JP. Binding of pyridoxal 5′-phosphate to the heme protein human cystathionine beta-synthase. Biochemistry. 1999; 38:2716–2724. [PubMed: 10052942]

Key BJ, White RP. Neuropharmacological comparison of cystathionine, cysteine, homoserine and alpha-ketobutyric acid in cats. Neuropharmacology. 1970; 9:349–357. [PubMed: 5456581]

Kinnunen A, Lintunen M, Karlstedt K, Fukui H, Panula P. In situ detection of H1-receptor mRNA and absence of apoptosis in the transient histamine system of the embryonic rat brain. J. Comp. Neurol. 1998; 394:127–137. [PubMed: 9550146]

Kraus JP, Hasek J, Kozich V, et al. Cystathionine gamma-lyase: Clinical, metabolic, genetic, and structural studies. Mol. Genet. Metab. 2009; 97:250–259. [PubMed: 19428278]

Kulak A, Duarte JM, Do KQ, Gruetter R. Neurochemical profile of the developing mouse cortex determined by in vivo 1H NMR spectroscopy at 14.1 T and the effect of recurrent anaesthesia. J. Neurochem. 2010; 115:1466–1477. [PubMed: 20946416]

Kulesskaya N, Voikar V, Peltola M, Yegutkin GG, Salmi M, Jalkanen S, Rauvala H. CD73 is a major regulator of adenosinergic signalling in mouse brain. PloS one. 2013; 8:e66896. [PubMed: 23776700]

Kurlemann G, Loscher W, Dominick HC, Palm GD. Disappearance of neonatal seizures and low CSF GABA levels after treatment with vitamin B6. Epilepsy Res. 1987; 1:152–154. [PubMed: 3504392]

Kurtz DJ, Levy H, Kanfer JN. Cerebral lipids and amino acids in the vitamin B 6 -deficient suckling rat. J. Nutr. 1972; 102:291–298. [PubMed: 5008749]

Lalande J, Halley H, Balayssac S, Gilard V, Dejean S, Martino R, Frances B, Lassalle JM, Malet-Martino M. 1H NMR metabolomic signatures in five brain regions of the AbetaPPswe Tg2576

mouse model of Alzheimer's disease at four ages. J Alzheimers Dis. 2014; 39:121–143. [PubMed: 24145382]

Lamers Y, Williamson J, Ralat M, et al. Moderate dietary vitamin B-6 restriction raises plasma glycine and cystathionine concentrations while minimally affecting the rates of glycine turnover and glycine cleavage in healthy men and women. J. Nutr. 2009; 139:452–460. [PubMed: 19158217]

Langer D, Hammer K, Koszalka P, Schrader J, Robson S, Zimmermann H. Distribution of ectonucleotidases in the rodent brain revisited. Cell Tissue Res. 2008; 334:199–217. [PubMed: 18843508]

Langer D, Ikehara Y, Takebayashi H, Hawkes R, Zimmermann H. The ectonucleotidases alkaline phosphatase and nucleoside triphosphate diphosphohydrolase 2 are associated with subsets of progenitor cell populations in the mouse embryonic, postnatal and adult neurogenic zones. Neuroscience. 2007; 150:863–879. [PubMed: 18031938]

Le GY, Essackjee HC, Ballard HJ. Intracellular adenosine formation and release by freshly-isolated vascular endothelial cells from rat skeletal muscle: effects of hypoxia and/or acidosis. Biochem. Biophys. Res. Commun. 2014; 450:93–98. [PubMed: 24866246]

Lima CP, Davis SR, Mackey AD, Scheer JB, Williamson J, Gregory JF 3rd. Vitamin B-6 deficiency suppresses the hepatic transsulfuration pathway but increases glutathione concentration in rats fed AIN-76A or AIN-93G diets. J. Nutr. 2006; 136:2141–2147. [PubMed: 16857832]

Linden DR, Sha L, Mazzone A, Stoltz GJ, Bernard CE, Furne JK, Levitt MD, Farrugia G, Szurszewski JH. Production of the gaseous signal molecule hydrogen sulfide in mouse tissues. J. Neurochem. 2008; 106:1577–1585. [PubMed: 18513201]

Litmanovitz, Reish O., Dolfin, T., Arnon, S., Regev, R., Grinshpan, G., Yamazaki, M., Ozono, K. Glu274Lys/Gly309Arg mutation of the tissue-nonspecific alkaline phosphatase gene in neonatal hypophosphatasia associated with convulsions. J. Inherit. Metab. Dis. 2002; 25:35–40. [PubMed: 11999978]

Liu J, Sheldon RA, Segal MR, Kelly MJS, Pelton JG, Ferriero DM, James TL, Litt L. 1H nuclear magnetic resonance brain metabolomics in neonatal mice after hypoxiaischemia distinguished normothermic recovery from mild hypothermia recoveries. Pediatr. Res. 2013; 74:170–179. [PubMed: 23708689]

Long CL, Dillard DR, Bodzin JH, Geiger JW, Blakemore WS. Validity of 3-methylhistidine excretion as an indicator of skeletal muscle protein breakdown in humans. Metabolism. 1988; 37:844–849. [PubMed: 3138511]

Long CL, Haverberg LN, Young VR, Kinney JM, Munro HN, Geiger JW. Metabolism of 3-methylhistidine in man. Metabolism. 1975; 24:929–935. [PubMed: 1143090]

Lott IT, Coulombe T, Di Paolo RV, Richardson EP Jr. Levy HL. Vitamin B6-dependent seizures: pathology and chemical findings in brain. Neurology. 1978; 28:47–54. [PubMed: 563538]

Lovatt D, Xu Q, Liu W, Takano T, Smith NA, Schnermann J, Tieu K, Nedergaard M. Neuronal adenosine release, and not astrocytic ATP release, mediates feedback inhibition of excitatory activity. Proceedings of the National Academy of Sciences of the United States of America. 2012; 109:6265–6270. [PubMed: 22421436]

Macdonald RL, Kang JQ, Gallagher MJ. Mutations in GABAA receptor subunits associated with genetic epilepsies. The Journal of physiology. 2010; 588:1861–1869. [PubMed: 20308251]

Mackiewicz M, Nikonova EV, Zimmermann JE, Romer MA, Cater J, Galante RJ, Pack AI. Age-related changes in adenosine metabolic enzymes in sleep/wake regulatory areas of the brain. Neurobiol. Aging. 2006; 27:351–360. [PubMed: 16399217]

Maitre M, Chesielski L, Lehmann A, Kempf E, Mandel P. Protective effect of adenosine and nicotinamide against audiogenic seizure. Biochem. Pharmacol. 1974; 23:2807–2816. [PubMed: 4154753]

Mandal R, Guo AC, Chaudhary KK, Liu P, Yallou FS, Dong E, Aziat F, Wishart DS. Multi-platform characterization of the human cerebrospinal fluid metabolome: a comprehensive and quantitative update. Genome medicine. 2012; 4:38. [PubMed: 22546835]

Martin DL, Martin SB, S.J. W, Espina N. Regulatory properties of brain glutamate decarboxylase (GAD) : the apoenzyme of GAD is present principally as the smaller of two molecular forms of GAD in brain. J Neurosci. 1991; 11:2725–2731. [PubMed: 1880546]

Martin DL, Rimvall K. Regulation of gamma-aminobutyric acid synthesis in the brain. J. Neurochem. 1993; 60:395–407. [PubMed: 8419527]

Martinez M, Cuskelly GJ, Williamson J, Toth JP, Gregory JF 3rd. Vitamin B-6 deficiency in rats reduces hepatic serine hydroxymethyltransferase and cystathionine beta-synthase activities and rates of in vivo protein turnover, homocysteine remethylation and transsulfuration. J. Nutr. 2000; 130:1115–1123. [PubMed: 10801907]

Masisi K, Suidasari S, Zhang P, Okazaki Y, Yanaka N, Kato N. Comparative study on the responses of concentrations of B(6)-vitamers in several tissues of mice to the dietary level of pyridoxine. J. Nutr. Sci. Vitaminol. (Tokyo). 2012; 58:446–451. [PubMed: 23419405]

Mason GF, Martin DL, Martin SB, Manor D, Sibson NR, Patel A, Rothman DL, Behar KL. Decrease in GABA synthesis rate in rat cortex following GABA-transaminase inhibition correlates with the decrease in GAD(67) protein. Brain research. 2001; 914:81–91. [PubMed: 11578600]

Matalon R, Rady PL, Platt KA, et al. Knock-out mouse for Canavan disease: a model for gene transfer to the central nervous system. The journal of gene medicine. 2000; 2:165–175. [PubMed: 10894262]

Mayahara H, Hirano H, Saito T, Ogawa K. The new lead citrate method for the ultracytochemical demonstration of activity of non-specific alkaline phosphatase (orthophosphoric monoester phosphohydrolase). Histochemie. 1967; 11:88–96. [PubMed: 5589645]

McCance RA, Morrison AB, Dent CE. The excretion of phosphoethanolamine and hypophosphatasia. Lancet. 1955; 268:131. [PubMed: 13222868]

Mori S, Nagano M. Electron microscopic cytochemistry of alkaline phosphatase in neurons of rats. Arch. Histol. Jpn. 1985; 48:389–397. [PubMed: 4084005]

Morre DM, Kirksey A, Das GD. Effects of vitamin B-6 deficiency on the developing central nervous system of the rat. Myelination. J. Nutr. 1978; 108:1260–1265. [PubMed: 671093]

Nakamura-Utsunomiya A, Okada S, Hara K, et al. Clinical characteristics of perinatal lethal hypophosphatasia: a report of 6 cases. Clinical pediatric endocrinology : case reports and clinical investigations : official journal of the Japanese Society for Pediatric Endocrinology. 2010; 19:7–13.

Namboodiri AM, Moffett JR, Arun P, et al. Defective myelin lipid synthesis as a pathogenic mechanism of Canavan disease. Advances in experimental medicine and biology. 2006; 576:145–163. discussion 361-143. [PubMed: 16802710]

Narisawa S, Frohlander N, Millan JL. Inactivation of two mouse alkaline phosphatase genes and establishment of a model of infantile hypophosphatasia. Dev. Dyn. 1997; 208:432–446. [PubMed: 9056646]

Narisawa S, Hasegawa H, Watanabe K, Millan JL. Stage-specific expression of alkaline phosphatase during neural development in the mouse. Dev. Dyn. 1994; 201:227–235. [PubMed: 7533563]

Narisawa S, Wennberg C, Millan JL. Abnormal vitamin B6 metabolism in alkaline phosphatase knock-out mice causes multiple abnormalities, but not the impaired bone mineralization. J. Pathol. 2001; 193:125–133. [PubMed: 11169525]

Negyessy L, Xiao J, Kantor O, et al. Layer-specific activity of tissue non-specific alkaline phosphatase in the human neocortex. Neuroscience. 2011; 172:406–418. [PubMed: 20977932]

Newman W, Feigin I, et al. Histochemical studies on tissue enzymes; distribution of some enzyme systems which liberate phosphate at pH 9.2 as determined with various substrates and inhibitors; demonstration of three groups of enzymes. Am J Pathol. 1950; 26:257–305. incl 257 pl. [PubMed: 15406255]

Nguyen TT, Hayakawa T, Tsuge H. Effect of vitamin B6 deficiency on the synthesis and accumulation of S-adenosylhomocysteine and S-adenosylmethionine in rat tissues. J. Nutr. Sci. Vitaminol. (Tokyo). 2001; 47:188–194. [PubMed: 11575573]

Nijhout HF, Gregory JF, Fitzpatrick C, Cho E, Lamers KY, Ulrich CM, Reed MC. A mathematical model gives insights into the effects of vitamin B-6 deficiency on 1-carbon and glutathione metabolism. J. Nutr. 2009; 139:784–791. [PubMed: 19244383]

Nisijima K, Ishiguro T. Cerebrospinal-Fluid Levels of Monoamine Metabolites and Gamma-Aminobutyric-Acid in Neuroleptic Malignant Syndrome. J. Psychiatr. Res. 1995; 29:233–244. [PubMed: 7473299]

Nordengen K, Heuser C, Rinholm JE, Matalon R, Gundersen V. Localisation of N-acetylaspartate in oligodendrocytes/myelin. Brain structure & function. 2015; 220:899–917. [PubMed: 24379086]

Nowak LG, Rosay B, Czege D, Fonta C. Tetramisole and Levamisole Suppress Neuronal Activity Independently from Their Inhibitory Action on Tissue Non-specific Alkaline Phosphatase in Mouse Cortex. Subcell. Biochem. 2015; 76:239–281. [PubMed: 26219715]

Nunes ML, Mugnol F, Bica I, Fiori RM. Pyridoxine-dependent seizures associated with hypophosphatasia in a newborn. J. Child Neurol. 2002; 17:222–224. [PubMed: 12026240]

Oh KJ, Churchich JE. Binding of pyridoxal 5-phosphate to cystathionase. The Journal of biological chemistry. 1973; 248:7370–7375. [PubMed: 4795694]

Ohkubo S, Kimura J, Matsuoka I. Ecto-alkaline phosphatase in NG108-15 cells : a key enzyme mediating P1 antagonist-sensitive ATP response. Br. J. Pharmacol. 2000; 131:1667–1672. [PubMed: 11139445]

Pagonopoulou O, Efthimiadou A, Asimakopoulos B, Nikolettos NK. Modulatory role of adenosine and its receptors in epilepsy: possible therapeutic approaches. Neurosci. Res. 2006; 56:14–20. [PubMed: 16846657]

Park YK, Linkswiler H. Effect of vitamin B6 depletion in adult man on the excretion of cystathionine and other methionine metabolites. J. Nutr. 1970; 100:110–116. [PubMed: 5412124]

Patel AB, de Graaf RA, Martin DL, Battaglioli G, Behar KL. Evidence that GAD65 mediates increased GABA synthesis during intense neuronal activity in vivo. J. Neurochem. 2006; 97:385–396. [PubMed: 16539672]

Percudani R, Peracchi A. The B6 database: a tool for the description and classification of vitamin B6-dependent enzymatic activities and of the corresponding protein families. BMC bioinformatics. 2009; 10:273. [PubMed: 19723314]

Picher M, Burch LH, Hirsh AJ, Spychala J, Boucher RC. Ecto 5′-nucleotidase and nonspecific alkaline phosphatase. Two AMP-hydrolyzing ectoenzymes with distinct roles in human airways. The Journal of biological chemistry. 2003; 278:13468–13479. [PubMed: 12560324]

Pike AF, Kramer NI, Blaauboer BJ, Seinen W, Brands R. An alkaline phosphatase transport mechanism in the pathogenesis of Alzheimer's disease and neurodegeneration. Chem. Biol. Interact. 2015; 226:30–39. [PubMed: 25500268]

Pinner B, Davison JF, Campbell JB. Alkaline phosphatase in peripheral nerves. Science. 1964; 145:936–938. [PubMed: 14163818]

Posen S, Whyte MP, Coburn SP, Freeman R, Collins F, Fedde KN, Bye A. Infantile hypophosphatasia with fatal status epilepticus. J Bone Miner Res. 1997; 12:S528.

Rathbun JC. Hypophosphatasia; a new developmental anomaly. Am. J. Dis. Child. 1948; 75:822–831. [PubMed: 18110134]

Regnier V, Billard JM, Gupta S, et al. Brain phenotype of transgenic mice overexpressing cystathionine beta-synthase. PloS one. 2012; 7:e29056. [PubMed: 22253703]

Robert K, Vialard F, Thiery E, Toyama K, Sinet PM, Janel N, London J. Expression of the cystathionine beta synthase (CBS) gene during mouse development and immunolocalization in adult brain. J. Histochem. Cytochem. 2003; 51:363–371. [PubMed: 12588964]

Robert O, Sabatier J, Desoubzdanne D, Lalande J, Balayssac S, Gilard V, Martino R, Malet-Martino M. pH optimization for a reliable quantification of brain tumor cell and tissue extracts with (1)H NMR: focus on choline-containing compounds and taurine. Anal Bioanal Chem. 2011; 399:987–999. [PubMed: 21069302]

Rodrigues RJ, Tome AR, Cunha RA. ATP as a multi-target danger signal in the brain. Frontiers in neuroscience. 2015; 9:148. [PubMed: 25972780]

Russell RG. Excretion of Inorganic Pyrophosphate in Hypophosphatasia. Lancet. 1965; 2:461–464. [PubMed: 14337825]

Sala-Newby GB, Skladanowski AC, Newby AC. The mechanism of adenosine formation in cells. Cloning of cytosolic 5′-nucleotidase-I. The Journal of biological chemistry. 1999; 274:17789–17793. [PubMed: 10364222]

Salek RM, Xia J, Innes A, Sweatman BC, Adalbert R, Randle S, McGowan E, Emson PC, Griffin JL. A metabolomic study of the CRND8 transgenic mouse model of Alzheimer's disease. Neurochem. Int. 2010; 56:937–947. [PubMed: 20398713]

Sato A, Nishioka M, Awata S, et al. Vitamin B6 deficiency accelerates metabolic turnover of cystathionase in rat liver. Arch. Biochem. Biophys. 1996; 330:409–413. [PubMed: 8660672]

Say JC, Ciuffi K, Furriel RP, Ciancaglini P, Leone FA. Alkaline phosphatase from rat osseous plates: purification and biochemical characterization of a soluble form. Biochim Biophys Acta. 1991; 1074:256–262. [PubMed: 2065078]

Schmitt B, vonBoth I, Amara CE, Schulze A. Quantitative Assessment of Metabolic Changes in the Developing Brain of C57BL/6 Mice by In Vivo Proton Magnetic Resonance Spectroscopy. J Alzheimers Dis Parkinsonism. 2013; 3(Issue 4):129. 1000129 3.

Schwartz JC, Rose C, Caillens H. Metabolism of methylhistamine formed through a new pathway: decarboxylation of L-3-methylhistidine. J. Pharmacol. Exp. Ther. 1973; 184:766–779. [PubMed: 4687236]

Shimizu N. Histochemical studies on the phosphatase of the nervous system. J. Comp. Neurol. 1950; 93:201–217. [PubMed: 14784516]

Sia C, Wapnir R, Sokal M, Harper RG, Intizar S, Manhasset F. Effects of pyridoxine on neonatal hypophosphatasia. Pediatr. Res. 1975; 9:355.

Sinclair AJ, Viant MR, Ball AK, Burdon MA, Walker EA, Stewart PM, Rauz S, Young SP. NMR-based metabolomic analysis of cerebrospinal fluid and serum in neurological diseases--a diagnostic tool? NMR Biomed. 2010; 23:123–132. [PubMed: 19691132]

Smolinska A, Blanchet L, Buydens LM, Wijmenga SS. NMR and pattern recognition methods in metabolomics: from data acquisition to biomarker discovery: a review. Anal. Chim. Acta. 2012; 750:82–97. [PubMed: 23062430]

Spector R. Vitamin B6 transport in the central nervous system: in vivo studies. J. Neurochem. 1978; 30:881–887. [PubMed: 650228]

Stephens MC, Dakshinamurti K. Brain lipids in pyridoxine-deficient young rats. Neurobiology. 1975; 5:262–269. [PubMed: 1202390]

Stephens MC, Havlicek V, Dakshinamurti K. Pyridoxine deficiency and development of the central nervous system in the rat. J. Neurochem. 1971; 18:2407–2416. [PubMed: 5135902]

Stevens B, Porta S, Haak LL, Gallo V, Fields RD. Adenosine: a neuron-glial transmitter promoting myelination in the CNS in response to action potentials. Neuron. 2002; 36:855–868. [PubMed: 12467589]

Stoop MP, Coulier L, Rosenling T, et al. Quantitative Proteomics and Metabolomics Analysis of Normal Human Cerebrospinal Fluid Samples. Mol Cell Proteomics. 2010; 9:2063–2075. [PubMed: 20811074]

Strauss KA, Morton DH, Puffenberger EG, et al. Prevention of brain disease from severe 5,10-methylenetetrahydrofolate reductase deficiency. Mol. Genet. Metab. 2007; 91:165–175. [PubMed: 17409006]

Street SE, Kramer NJ, Walsh PL, et al. Tissue-nonspecific alkaline phosphatase acts redundantly with PAP and NT5E to generate adenosine in the dorsal spinal cord. J Neurosci. 2013; 33:11314–11322. [PubMed: 23825434]

Street SE, Sowa NA. TNAP and Pain Control. Subcell. Biochem. 2015; 76:283–305. [PubMed: 26219716]

Sugimura K, Mizutani A. Histochemical and cytochemical studies of alkaline phosphatase activity in the synapses of rat brain. Histochemistry. 1979; 61:123–129. [PubMed: 457450]

Taillandier A, Sallinen SL, Brun-Heath I, De Mazancourt P, Serre JL, Mornet E. Childhood hypophosphatasia due to a de novo missense mutation in the tissue-nonspecific alkaline phosphatase gene. J. Clin. Endocrinol. Metab. 2005; 90:2436–2439. [PubMed: 15671102]

Taketani T. Neurological Symptoms of Hypophosphatasia. Subcell. Biochem. 2015; 76:309–322. [PubMed: 26219717]

Taketani T, Onigata K, Kobayashi H, Mushimoto Y, Fukuda S, Yamaguchi S. Clinical and genetic aspects of hypophosphatasia in Japanese patients. Arch. Dis. Child. 2014; 99:211–215. [PubMed: 24276437]

Taoka S, Widjaja L, Banerjee R. Assignment of enzymatic functions to specific regions of the PLP-dependent heme protein cystathionine beta-synthase. Biochemistry. 1999; 38:13155–13161. [PubMed: 10529187]

Traut TW. Physiological Concentrations of Purines and Pyrimidines. Mol. Cell. Biochem. 1994; 140:1–22. [PubMed: 7877593]

van Belle H. Kinetics and inhibition of rat and avian alkaline phosphatases. Gen. Pharmacol. 1976; 7:53–58. [PubMed: 9334]

Vorbrodt AW, Lossinsky AS, Wisniewski HM. Localization of alkaline phosphatase activity in endothelia of developing and mature mouse blood-brain barrier. Dev. Neurosci. 1986; 8:1–13. [PubMed: 3743466]

Wall MJ, Dale N. Neuronal transporter and astrocytic ATP exocytosis underlie activity-dependent adenosine release in the hippocampus. The Journal of physiology. 2013; 591:3853–3871. [PubMed: 23713028]

Wasynczuk A, Kirksey A, Morre DM. Effect of maternal vitamin B-6 deficiency on specific regions of developing rat brain: amino acid metabolism. J. Nutr. 1983; 113:735–745. [PubMed: 6834146]

Watanabe, T., Taguchi, Y., Maeyama, K., Wada, H. Formation of histamine: histidine decarboxylase. In: Uvna¨s, B., editor. Handbook of experimental pharmacology. Vol. Vol. 97. Springer Verlag; Berlin: 1991. p. 145-163.

Waymire KG, Mahuren JD, Jaje JM, Guilarte TR, Coburn SP, MacGregor GR. Mice lacking tissue non-specific alkaline phosphatase die from seizures due to defective metabolism of vitamin B-6. Nat. Genet. 1995; 11:45–51. [PubMed: 7550313]

Weiss MJ, Ray K, Henthorn PS, Lamb B, Kadesch T, Harris H. Structure of the human liver/bone/kidney alkaline phosphatase gene. The Journal of biological chemistry. 1988; 263:12002–12010. [PubMed: 3165380]

Werman R, Davidoff RA, Aprison MH. The inhibitory action of cystathionine. Life Sci. 1966; 5:1431–1440. [PubMed: 5968707]

Whyte MP, Mahuren JD, Fedde KN, Cole FS, McCabe ER, Coburn SP. Perinatal hypophosphatasia: tissue levels of vitamin B6 are unremarkable despite markedly increased circulating concentrations of pyridoxal-5′-phosphate. Evidence for an ectoenzyme role for tissue-nonspecific alkaline phosphatase. The Journal of clinical investigation. 1988; 81:1234–1239. [PubMed: 3350970]

Whyte MP, Mahuren JD, Vrabel LA, Coburn SP. Markedly increased circulating pyridoxal-5′-phosphate levels in hypophosphatasia. Alkaline phosphatase acts in vitamin B6 metabolism. The Journal of clinical investigation. 1985; 76:752–756. [PubMed: 4031070]

Wishart DS, Jewison T, Guo AC, et al. HMDB 3.0--The Human Metabolome Database in 2013. Nucleic Acids Res. 2013; 41:D801–807. [PubMed: 23161693]

Wishart DS, Lewis MJ, Morrissey JA, et al. The human cerebrospinal fluid metabolome. Journal of chromatography. B, Analytical technologies in the biomedical and life sciences. 2008; 871:164–173. [PubMed: 18502700]

Wolf NI, Willemsen MA, Engelke UF, et al. Severe hypomyelination associated with increased levels of N-acetylaspartylglutamate in CSF. Neurology. 2004; 62:1503–1508. [PubMed: 15136672]

Yamamoto H, Sasamoto Y, Miyamoto Y, Murakami H, Kamiyama N. A successful treatment with pyridoxal phosphate for West syndrome in hypophosphatasia. Pediatr. Neurol. 2004; 30:216–218. [PubMed: 15033207]

Yang G, Wu L, Jiang B, et al. H2S as a physiologic vasorelaxant: hypertension in mice with deletion of cystathionine gamma-lyase. Science. 2008; 322:587–590. [PubMed: 18948540]

Yang Y, Wandler AM, Postlethwait JH, Guillemin K. Dynamic Evolution of the LPSDetoxifying Enzyme Intestinal Alkaline Phosphatase in Zebrafish and Other Vertebrates. Frontiers in immunology. 2012; 3:314. [PubMed: 23091474]

Young VR, Alexis SD, Baliga BS, Munro HN, Muecke W. Metabolism of administered 3-methylhistidine. Lack of muscle transfer ribonucleic acid charging and quantitative excretion as 3-methylhistidine and its N-acetyl derivative. The Journal of biological chemistry. 1972; 247:3592–3600. [PubMed: 5030632]

Zhang D, Xiong W, Chu S, Sun C, Albensi BC, Parkinson FE. Inhibition of hippocampal synaptic activity by ATP, hypoxia or oxygen-glucose deprivation does not require CD73. PloS one. 2012; 7:e39772. [PubMed: 22761898]

Zimmermann H. Nucleotide signaling in nervous system development. Pflugers Arch. 2006; 452:573–588. [PubMed: 16639549]

Zimmermann H, Zebisch M, Strater N. Cellular function and molecular structure of ectonucleotidases. Purinergic signalling. 2012; 8:437–502. [PubMed: 22555564]

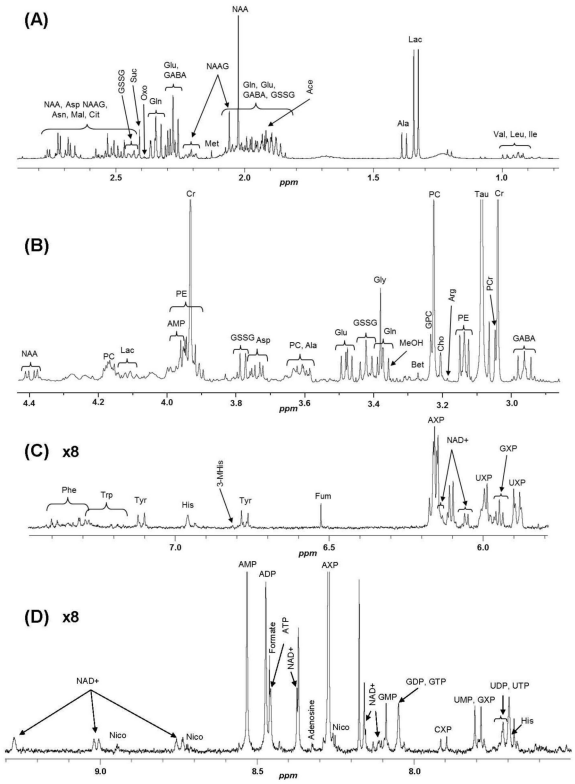

Figure 1

^{1}H NMR spectrum of an aqueous extract of the brain from an *Akp2*$^{+/+}$ mouse. **(A)** 2.9-0.8 ppm region, (**B**) 4.4-2.9 ppm region, (**C**) 7.5-5.65 ppm region, (**D**) 9.3-7.5 ppm region. (A) and (B) regions of the spectrum: valine (Val), isoleucine (Ile), leucine (Leu), lactate (Lac), alanine (Ala), glutamate (Glu), glutamine (Gln), oxoproline (Oxo), γ-aminobutyric acid (GABA), acetate (Ace), glutathione disulfide (GSSG), N-acetylaspartate (NAA), N-acetyl-aspartyl-glutamate (NAAG), succinate (Suc), aspartate (Asp), citrate (Cit), asparagine (Asn), malate (Mal), creatine (Cr), phosphocreatine (PCr), taurine (Tau), phosphoethanolamine (PE), choline (Cho), phosphocholine (PC), glycerophosphocholine (GPC), betaine (Bet) and glycine (Gly). Methanol (MeOH) is a residual solvent. (C) and (D) regions of the spectrum: nicotinamide adenine dinucleotide (NAD^{+}), adenosine diphosphate (ADP), nicotinamide (Nico), adenosine monophosphate (AMP), adenine (Ade), adenosine mono-, di- and triphosphate (AXP), guanosine triphosphate (GTP), guanosine diphosphate (GDP), guanosine monophosphate (GMP), guanosine mono-, di- and triphosphate (GXP), uridine triphosphate (UTP), uridine diphosphate (UDP), uridine monophosphate (UMP), uridine mono-, di- and triphosphate (UXP), cytidine mono-, di- and triphosphate (CXP), phenylalanine (Phe), tryptophan (Trp), tyrosine (Tyr), histidine (His), 3-methylhistidine (3-MHis), fumarate (Fum). Peaks for the most abundant compounds (Tau and Cr) have been truncated.

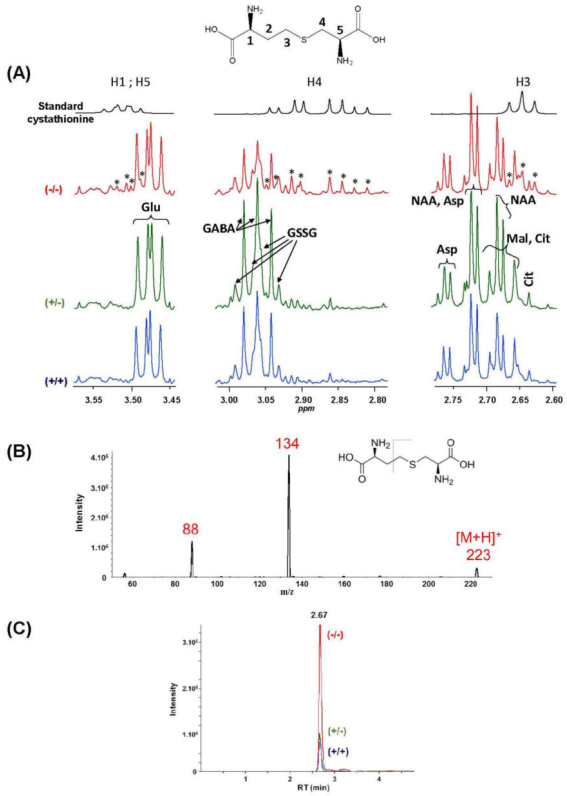

Figure 2.

(A) Comparison of ^{1}H NMR spectra (zooms around 2.7, 2.9 and 3.5 ppm) of a solution of standard cystathionine and of aqueous brain extracts from *Akp2*$^{+/+}$ (blue), *Akp2*$^{+/-}$ (green) and *Akp2*$^{-/-}$ (red) mice. *: signals fitting with those of cystathionine standard. Abbreviations of metabolites: see caption of Figure 1. **(B)** Full scan MS spectrum of standard cystathionine. **(C)** UHPLC-MS/MS chromatograms by SRM (223 →134 transition).

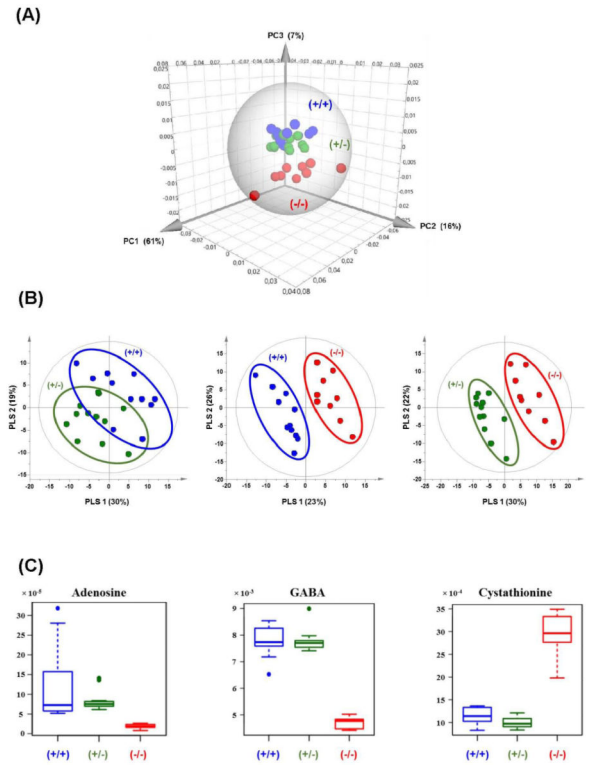

Figure 3.

(A) Three-dimensional score plot of PCA on the NMR data collected from all brain extracts. The confidence ellipse (Hotelling's T2) defines the region that contains 99% of the data. **(B)** Score plots of the PLS-DA on NMR data of *Akp2*$^{+/+}$ versus *Akp2*$^{+/-}$ mice, *Akp2*$^{+/+}$ versus *Akp2*$^{-/-}$ mice and *Akp2*$^{+/-}$ versus *Akp2*$^{-/-}$ mice. **(C)** Boxplots for adenosine (singulet at 8.33 ppm), GABA (triplet at 2.29 ppm) and cystathionine (triplet at 2.65 ppm). The ordinates of the boxplots represent normalized areas of NMR signals. *Akp2*$^{+/+}$ are shown in blue, *Akp2*$^{+/-}$ in green and *Akp2*$^{-/-}$ in red.

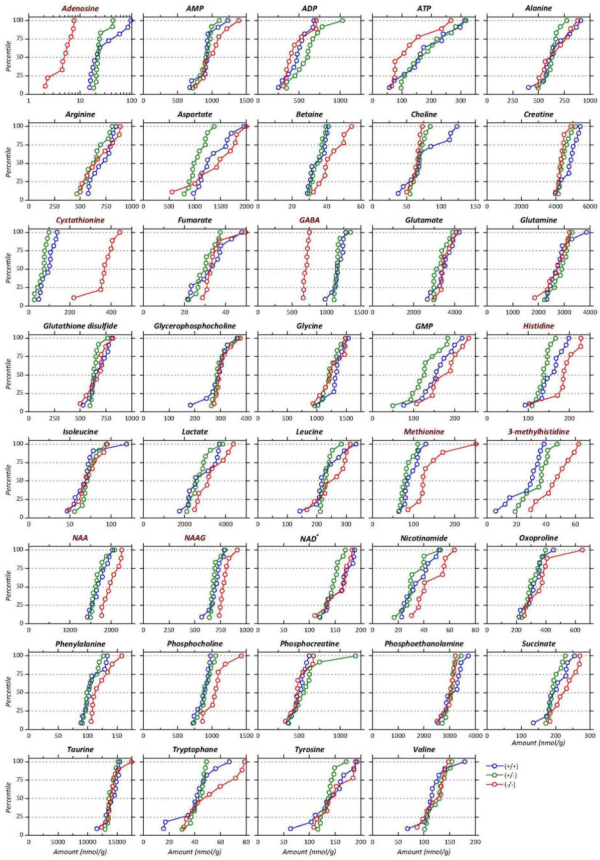

Figure 4.

Cumulative distributions of the concentrations of the 39 metabolites identified for the 3 groups of mice: $Akp2^{+/+}$ (blue), $Akp2^{+/-}$ (green) and $Akp2^{-/-}$ (red). Metabolites have been ordered alphabetically. Names in red correspond to metabolites whose concentration differed significantly between $Akp2^{-/-}$ and $Akp2^{+/+}$ and $^{+/-}$ mice. Note log scale for adenosine.

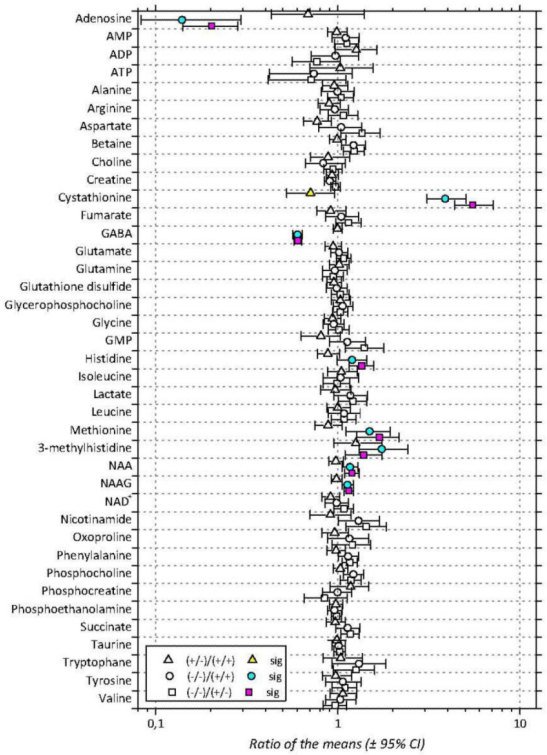

Figure 5.

Ratios of the mean concentrations for the 39 metabolites identified in aqueous extracts of $Akp2^{+/+}$ (+/+), $Akp2^{+/-}$ (+/−) and $Akp2^{-/-}$ (-/-) mice brains. Symbols correspond to the actual ratio and bars encompass the 95% confidence interval of the ratio. Triangles represent the $Akp2^{+/-}/Akp2^{+/+}$ ratios, squares the $Akp2^{-/-}/Akp2^{+/-}$ ratios and circles the $Akp2^{-/-}/Akp2^{+/+}$ ratios. Colored symbols indicate significant differences ($p<0.05$) between $Akp2^{-/-}$ and $Akp2^{+/+}$ (cyan), $Akp2^{+/-}$ and $Akp2^{+/+}$ (yellow) and $Akp2^{-/-}$ and $Akp2^{+/-}$ (magenta) mice. Significant differences are typically associated to 95% confidence intervals that do not straddle the unity ratio value.

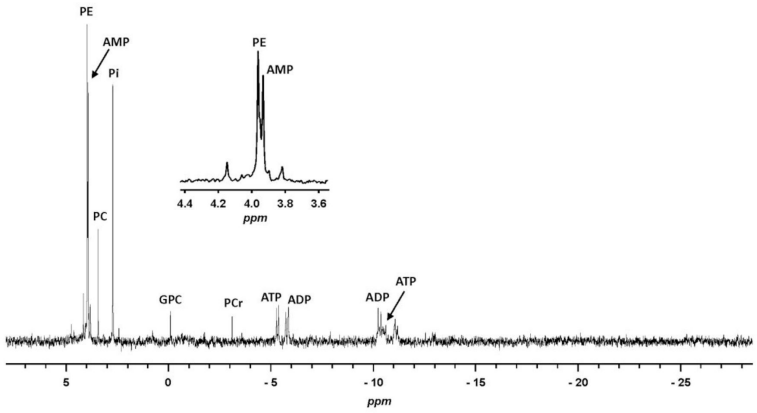

Figure 6.

^{31}P NMR spectrum of an aqueous extract of a mouse brain with an *Akp2*$^{+/+}$ phenotype. PE: phosphoethanolamine; PC: phosphocholine; AMP: adenosine monophosphate; Pi: inorganic phosphate; GPC: glycerophosphocholine; PCr: phosphocreatine; ATP: adenosine triphosphate; ADP: adenosine diphosphate (ADP).

Table 1

Concentrations, along with the considered NMR signals, of the 39 metabolites identified in aqueous brain extracts of Akp2$^{+/+}$ (+/+), Akp2$^{+/-}$ (+/−), and Akp2$^{-/-}$ (−/−) mice brains (s: singlet; d: doublet; dd: doublet of doublet; t: triplet; m: multiplet). The 8 discriminating metabolites are shown at the top of the table (bold), followed by the 31 other metabolites alphabetically listed. The mean concentrations and standard deviations (SD) are expressed in nmol/g of wet brain tissue. Variations were calculated with the mean concentration values (CI: 95% confidence interval).

Metabolites	NMR signals considered for quantification (δ, multiplicity)	Mean concentration nmol/g (SD)			Variation Ratio of the means [CI low-CI high]		
					−/−		+/−
		+/+	+/−	−/−	*vs* +/+	*vs* +/−	*vs* +/+
Adenosine	8.327 (s)	37 (29)	25 (8)	5 (2)	0.14 [0.08-0.29]	0.20 [0.14-0.28]	0.69 [0.43-1.40]
Cystathionine	2.884 (ABd system)[a]	94 (31)	67 (23)	366 (62)	3.89 [3.10-5.05]	5.49 [4.36-7.14]	0.71 [0.52-0.96]
GABA	2.288 (t)	1169 (87)	1 165 (64)	702 (33)	0.60 [0.57-0.64]	0.60 [0.58-0.63]	1,00 [0.94-1.06]
Methionine	2.127 (s)	94 (19)	83 (16)	141 (48)	1.50 [1.11-1.93]	1.69 [1.27-2.16]	0.89 [0.75-1.05]
3-methylhistidine	6.810 (s)	27 (11)	34 (9)	47 (11)	1.75 [1.31-2.43]	1.39 [1.10-1.75]	1.26 [0.95-1.74]
Histidine	6.955 (s)	156 (31)	138 (16)	187 (37)	1.20 [0.99-1.44]	1.36 [1.15-1.57]	0.88 [0.77-1.02]
NAA	2.024 (s)	1 719 (199)	1 680 (173)	2 010 (192)	1.17 [1.06-1.29]	1.20 [1.09-1.31]	0.98 [0.89-1.08]
NAAG	2.058 (s)	702 (63)	691 (43)	794 (54)	1.13 [1.05-1.22]	1.15 [1.08-1.22]	0.99 [0.92-1.06]
AMP	8.532 (s)	925 (152)	913 (103)	1 023 (194)	1.11 [0.93-1.31]	1.12 [0.96-1.29]	0.99 [0.88-1.12]
ADP	8.473 (s)	479 (137)	605 (190)	465 (152)	0.97 [0.71-1.30]	0.77 [0.56-1.03]	1.26 [0.97-1.64]
ATP	8.458 (s)	179 (85)	185 (76)	132 (74)	0.74 [0.42-1.20]	0.71 [0.42-1.11]	1.03 [0.70-1.57]
Alanine	1.379 (d)	662 (150)	633 (75)	662 (143)	1,00 [0.81-1.23]	1.05 [0.88-1.23]	0.96 [0.82-1.13]
Arginine	3.186 (t) [a]	715 (102)	641 (112)	688 (150)	0.96 [0.80-1.14]	1.07 [0.89-1.29]	0.90 [0.78-1.03]
Aspartate	3.740 (dd) [a]	1 370 (311)	1 055 (174)	1 432 (462)	1.05 [0.78-1.35]	1.36 (1.04-1.71]	0.77 (0.65-0.92]
Betaine	3.271 (s)	35 (5)	35 (3)	43 (7)	1.22 [1.05-1.42]	1.23 [1.07-1.40]	0.99 [0.90-1.10]

Metabolites	NMR signals considered for quantification (δ, multiplicity)	Mean concentration nmol/g (SD)			Variation Ratio of the means [CI low-CI high]		
					−/−		+/−
		+/+	+/−	−/−	*vs* +/+	*vs* +/−	*vs* +/+
Choline	3.205 (s)	77 (29)	68 (9)	64 (7)	0.83 [0.66-1.10]	0.94 [0.84-1.05]	0.89 [0.71-1.17]
Creatine	3.039 (s)	4 813 (467)	4 485 (321)	4 355 (255)	0.91 [0.84-0.98]	0.97 [0.92-1.03]	0.93 [0.87-1.01]
Fumarate	6.524 (s)	33 (8)	30 (5)	35 (6)	1.05 [0.86-1.29]	1.15 [0.98-1.34]	0.91 [0.76-1.11]
Glutamate	2.277 (t)	3 477 (461)	3 279 (331)	3 531 (325)	1.02 [0.92-1.13]	1.08 [0.99-1.18]	0.94 [0.85-1.05]
Glutamine	2.344 (m)	2 805 (453)	2 859 (333)	2 703 (434)	0.96 [0.83-1.12]	0.95 [0.83-1.08]	1.02 [0.90-1.16]
Glutathione disulfide	3.783 (AB system) [a]	676 (88)	645 (45)	667 (97)	0.99 [0.86-1.12]	1.04 [0.92-1.15]	0.95 [0.87-1.05]
Glycerophosphocholine	3.23.4 (s)	289 (47)	299 (30)	308 (32)	1.06 [0.94-1.21]	1.03 [0.94-1.13]	1.03 [0.92-1.17]
Glycine	3.380 (s)	1 321 (149)	1 237 (149)	1 256 (197)	0.95 [0.83-1.08]	1.02 [0.89-1.16]	0.94 [0.85-1.04]
GMP	8.091 (s)	157 (40)	127 (38)	177 (40)	1.13 [0.90-1.42]	1.40 [1.10-1.79]	0.81 [0.63-1.03]
Isoleucine	0.975 (d) [a]	70 (19)	74 (10)	73 (15)	1.04 [0.83-1.30]	0.99 [0.83-1.16]	1.05 [0.88-1.28]
Lactate	1.333 (d)	2 823 (707)	2 740 (499)	3 315 (682)	1.17 [0.95-1.46]	1.21 (1.00-1.46]	0.97 [0.81-1.19]
Leucine	0.925 (d) [a]	234 (52)	234 (020)	254 (52)	1.09 [0.89-1.33]	1.09 [0.92-1.26]	1.00 [0.87-1.17]
NAD^+	8.748 (d), 9.013 (d) and 9.273 (s)	160 (24)	146 (15)	157 (25)	0.99 [0.85-1.14]	1.08 [0.95-1.22]	0.91 [0.82-1.02]
Nicotinamide	8.716 (dd) and 8.946 (d)	35 (10)	32 (9)	46 (12)	1.30 [1.00-1.70]	1.43 [1.11-1.84]	0.91 [0.70-1.18]
Oxoproline	2.387 (m)	323 (67)	311 (53)	374 (117)	1.16 [0.88-1.48]	1.21 [0.93-1.51]	0.96 [0.82-1.14]
Phenylalanine	7.348 (m)	108 (16)	106 (12)	123 (18)	1.14 [1.01-1.30]	1.16 [1.06-1.28]	0.98 [0.87-1.10]
Phosphocholine	3.225 (s)	879 (88)	907 (98)	1 072 (171)	1.22 [1.07-1.38]	1.18 [1.03-1.34]	1.03 [0.94-1.13]
Phosphocreatine	3.046 (s)	506 (78)	596 (216)	504 (112)	1,00 [0.82-1.19]	0.85 [0.65-1.13]	1.18 [0.91-1.47]
Phosphoethanolamine	3.136 (m)	3 129 (371)	3 056 (192)	3 003 (230)	0.96 [0.88-1.05]	0.98 [0.92-1.05]	0.98 [0.90-1.06]

Metabolites	NMR signals considered for quantification (δ, multiplicity)	Mean concentration nmol/g (SD)			Variation Ratio of the means [CI low-CI high]		
					−/−		+/−
		+/+	+/−	−/−	*vs* +/+	*vs* +/−	*vs* +/+
Succinate	2.407 (s)	201 (34)	195 (18)	228 (34)	1.13 [0.98-1.32]	1.17 [1.04-1.31]	0.97 [0.86-1.10]
Taurine	3.085 (s)	14 153 (1 206)	13 996 (666)	14 312 (1 401)	1.01 [0.93-1.10]	1.02 [0.95-1.10]	0.99 [0.93-1.05]
Tryptophane	7.183 (m) and 7.530 (m)	41 (15)	43 (6)	54 (19)	1.31 [0.92-1.84]	1.26 [0.94-1.59]	1.04 [0.83-1.36]
Tyrosine	6.771 and 7.107 (AA'XX' system)	141 (38)	138 (15)	150 (31)	1.07 [0.86-1.34]	1.09 [0.93-1.27]	0.98 [0.82-1.19]
Valine	0.989 (d)	118 (27)	126 (18)	122 (21)	1.03 [0.86-1.25]	0.97 [0.83-1.12]	1.07 [0.91-1.27]

[a]Only a part of the signal was considered for quantification.

Table 2

Statistical comparisons of the mean concentrations of the 8 discriminating metabolites between $Akp2^{+/+}$, $Akp2^{-/-}$ and $Akp2^{+/-}$ genotypes (non-parametric tests, with correction for multiple comparisons).

Metabolites	p-values			
	Kruskal-Wallis	*Mann-Whitney*		
		−/− *vs.* +/+	−/− *vs.* +/−	+/− *vs.* +/+
Adenosine	$2.4\ 10^{-3}$	$4.0\ 10^{-4}$	$3.0\ 10^{-4}$	
Cystathionine	$3.0\ 10^{-5}$	$4.0\ 10^{-4}$	$3.0\ 10^{-4}$	$4.2\ 10^{-2}$
GABA	$1.4\ 10^{-4}$	$4.0\ 10^{-4}$	$3.0\ 10^{-4}$	
Methionine	$2.1\ 10^{-3}$	$6.8\ 10^{-3}$	$1.2\ 10^{-3}$	
3-methylhistidine	$1.4\ 10^{-2}$	$8.1\ 10^{-3}$	$2.1\ 10^{-2}$	
Histidine	$2.9\ 10^{-2}$	$4.9\ 10^{-2}$	$8.4\ 10^{-3}$	
NAA	$4.6\ 10^{-2}$	$2.2\ 10^{-2}$	$8.4\ 10^{-3}$	
NAAG	$4.7\ 10^{-3}$	$4.2\ 10^{-3}$	$2.4\ 10^{-3}$	